INCOMING RADIATION

AND VERTICAL TEMPERATURE PROFILES

IN A POLLUTED URBAN ATMOSPHERE

INCOMING RADIATION
AND VERTICAL TEMPERATURE PROFILES
IN A POLLUTED URBAN ATMOSPHERE

by

DONALD VICTOR NOAD, B.Sc.

A Thesis

Submitted to the Faculty of Graduate Studies

in Partial Fulfillment of the Requirements

for the Degree

Master of Science

McMaster University

April 1973

MASTER OF SCIENCE (1973)
(Geography)

McMaster University
Hamilton, Ontario

TITLE: Incoming Radiation and Vertical Temperature Profiles in a Polluted Urban Atmosphere

AUTHOR: Donald Victor Noad, B.Sc. (McMaster University)

SUPERVISOR: Dr. W.R. Rouse

NUMBER OF PAGES: vii, 54

SCOPE AND CONTENTS:

Simultaneous measurements of incoming short and longwave radiation were made at a rooftop site in the industrial heart of Hamilton, Ontario, and at a control station several miles to the south of the city at Mt. Hope airport. Direct comparison of these measurements was facilitated by selecting clear sky days from the winter solstice to the end of April.

Results indicate that the decrease in solar radiation intensity due to atmospheric pollution is balanced by a comparable increase in the flux of incoming longwave radiation from the sky. Receipts of total incoming radiation are therefore the same at both sites.

Vertical air temperature profiles over the industrial site and the control site were measured using a specially designed aircraft-mounted sensor. Profiles were determined on the same days that radiation measurements were made.

While the temperature profiles at the control site occasionally exhibited a slight subsidence inversion, the industrial profiles consistently showed a marked inversion whose magnitude diminished with increasing solar altitude and increased again toward sunset. This behaviour

is attributed to the enhanced shortwave absorptivity and longwave emissivity properties of the polluted atmosphere.

The height of the inversion increased during the morning hours and fell again during the afternoon in response to atmospheric convection caused by surface and atmospheric heating during the day. The top of the inversion, however, always coincided exactly with the top of the visible pollution dome.

ACKNOWLEDGEMENTS

This thesis incorporates the efforts of several people. I am indebted to my supervisor, Dr. W.R. Rouse, for the generous guidance, thoughtful ideas, and the monetary resources which he provided for the project. My thanks are also extended to Mr. John McCutcheon for teaching me the operation of the instruments and recorders, as well as for the use of a computer program which he originally developed.

TABLE OF CONTENTS

LIST OF FIGURES

LIST OF TABLES

CHAPTER I

OBJECTIVE, HYPOTHESIS AND APPROACH

1. Objective

The purpose of this study is to understand the effect of heavy concentrations of urban aerosols in Hamilton on the incoming shortwave and longwave radiation regimes and the influence of the radiative behaviour on the vertical temperature structure of the urban atmosphere.

2. Hypothesis

From the prior work of Rouse and McCutcheon (1972) in Hamilton it was postulated that the additional attenuation of global solar radiation in an industrial atmosphere is partly due to the absorption of radiation by the atmospheric aerosols. This suggests that the rate of atmospheric heating of an industrially polluted area will be greater than that over an unpolluted area and that this extra heating will result in an increased longwave radiation flux to the ground.

In addition this increase in the downward infrared flux in an industrialized area should be partly attributable to the higher emissivities of particulate and gaseous materials in the urban/industrial atmosphere.

3. Approach

This study was pursued in the city of Hamilton, Ontario and the adjacent rural area. Radiation measurements were made at rooftop sites in

the heart of the industrial area and the rural surroundings. Vertical temperature profiles were obtained using a sensor especially designed for use on a fixed-wing aircraft.

CHAPTER II

THEORY AND LITERATURE REVIEW

1. The Radiation Balance

The general expression for the radiation balance at the surface is

$$R_n = (Q + q) - RG + L_i - L_o$$

where R_n is the net radiation,

$(Q+q)$ is the total incoming shortwave flux,

RG is the outgoing shortwave reflected from the surface,

L_i is the incoming longwave flux, and

L_o is the outgoing longwave flux.

The total incoming shortwave flux, $(Q+q)$, is composed of two parts: Q represents the direct beam solar radiation, and q represents that portion of the total shortwave flux due to diffuse shortwave radiation.

The magnitude of the incoming longwave flux, L_i, is a function of the temperature and the radiative emissivity of the atmosphere.

Any substance whose temperature exceeds absolute zero (0°K or -273°C) will radiate according to the Stefan-Boltzmann Law,

$$E = \sigma \varepsilon T^4$$

where E is the radiant energy flux emitted by a body,

σ is the Stefan-Boltzmann constant, and

T is the absolute temperature of the body.

The emissivity, ε, is a measure of the efficiency of a radiating substance, relative to an ideal radiator or "black body" at the same temperature. It is a function of the nature of that substance.

2. Radiative and Temperature Effects of Atmospheric Pollutants

A. The Attenuation of Solar Radiation

The depletion of incoming solar radiation by airborne pollutants has been observed by a number of investigators. An early study by Hand (1949) was concerned with comparing the incoming radiation (total direct and diffuse radiation) in the smoke-contaminated business section of Boston with the incoming radiation experienced at Blue Hill Observatory, located on the top of the highest peak of the Blue Hills, 10 miles S/SW of the urban location. The total shortwave radiation received on a horizontal surface in downtown Boston was only 82% of that received at Blue Hill as measured over a 4-year period.

Hand's results also indicated increasing attenuation in early morning and late afternoon periods. This was due to the influence exerted by the increased air mass through which solar radiation must pass as the zenith angle became larger.

An examination of the seasonal variation in the amount of radiation attenuation by pollutants reported by Hand reveals that the highest rates of depletion occurred in December and January. This corresponded to the

high coal and oil smoke levels resulting from the increased demand for space heating during these two months.

Other workers who have noted strong attenuation of solar radiation in polluted urban atmospheres include Mateer (1961), working in Toronto, who found that there was less radiation depletion on Sundays than on work days during 20 years of radiation measurements. East (1967) working in Montreal reported typical attenuation values of 10 to 20%. Sekiguti (1964) noted that the downtown core of Inas, a small industrial city in central Japan, received less solar radiation than the outskirts. Finally, Bach and Patterson (1969) found depletion of solar radiation occurring in Cincinnati.

Recently, Rouse and McCutcheon (1972) demonstrated that there is a substantially greater attenuation of sunlight in the industrial atmosphere of Hamilton, Ontario, than for a control site. This effect begins immediately at sunrise and persists until sunset. For all measurements the attenuation averaged 9%. Ignoring the early morning and late evening hours when the measurements become unreliable the maximum attenuation of solar radiation was found to be 17%.

Idso (1972) reported on a series of global radiation measurements taken during a major desert dust storm on an otherwise clear day. These results were compared to a set of measurements taken at the same time of year on clear sky days in the absence of dust storm conditions. In general, incoming solar radiation was depleted by 22% during the storm activity.

The increased attenuation of shortwave radiation observed under

pollution conditions is the result of several processes. In a pollution layer, the general coefficient of attenuation, a_λ, may be considered as the sum

$$a_\lambda = a_{m\lambda} + a_{r\lambda} + a_{abs\lambda}$$

where $a_{m\lambda}$ is the coefficient for Mie scattering

$a_{r\lambda}$ is the coefficient for Rayleigh scattering, and

$a_{abs\lambda}$ is the coefficient of absorption.

The general attenuation coefficient of a collection of suspended matter of any size distribution decreases with increasing wavelength. Direct measurements in the cloud-free atmosphere yield the empirical relationship

$$a_\lambda = \omega\lambda^{-\beta}$$

where λ is the wavelength, and ω is the concentration of particles. β varies inversely with particle size such that in fog or mist $\beta \simeq 0$ and under very clear conditions $\beta \simeq 2$ (Leighton, 1961).

The dominance of absorption over scattering for urban/industrial haze was found by Lettau and Lettau (1969) using data from Robinson (1962). In their example, the attenuating properties of the contamination over Kew, England, were compared to those of natural impurities in the air such as mineral dust at La Joya, Peru (a desert site) and O'Neill, Nebraska (a prairie location). While the total attenuation due to particulate matter is roughly the same for each particle type, the ratio of absorption/scattering is about 4/3 for the city, 2/3 for the desert, and 3/3 or unity

for the prairie land.

Lettau's computations showed that by increasing the urban/industrial pollution concentration, the quantity of energy absorbed, the heating rate of the air, and the ratio of diffuse/direct radiation all increased dramatically. This contrasted markedly to the developments which took place when desert and prairie dust concentrations were increased. In this situation, the changes were comparatively minor.

B. The Elevated Heating Layer

Absorption is one of the major attenuating processes in the short-wave part of the spectrum. The absorption of sunlight by a layer of high turbidity would create strong atmospheric heating in that layer, as shown by Lettau and Lettau (1969). It follows that the heating due to the absorption of sunlight should result in a temperature anomaly in the zone of pollution. This possibility has been noted by both Atwater (1971) and Bergstrom (1971).

The heating rates which occur in heavily polluted areas are substantial. Roach (1961) suggested that heating rates greater than 10C°/day (about 0.5C°/hour) may occur; the gas NO_2, at a concentration of 1 ppm, is capable of producing heating rates of 30C°/day at solar noon (Atwater, 1971). Although the normal concentration of NO_2 under natural conditions is about 0.02 ppm, concentrations of 1.0 ppm are commonly observed in urban/industrial pollution conditions (Tebbens, 1968). The rates quoted by Atwater would never be observed in nature since radiative cooling and convective heat exchange with surrounding air layers would be initiated immediately.

C. The Increase in Longwave Radiation to the Surface

The creation of an elevated heating layer implies that an increase in the longwave flux to the earth should be present. Such an effect was found by Conaway and van Bavel (1967), although their instrumental techniques were criticized by Idso and Jackson (1968). In their examination of sky radiant emittance on cloudless days near Phoenix, they found fluctuations in the incoming longwave flux which were closely correlated with increases in the concentration of ozone from industrial sources. (Effects caused by CO_2 and H_2O vapour fluctuations were eliminated by using a selective spectral region bandpass.) Conaway and van Bavel also postulated that an air pollutant other than O_3 could be contributing to the measured effects.

In his study of the influence of the desert dust storm on radiation intensities, Idso (1972) noted that as the magnitude of shortwave radiation attenuation increased, the incoming longwave received at the surface increased by an average of 12.5% above measurements made on comparable clear sky days during daylight hours. This increase was attributed to significantly higher emissivities for dust particles.

In their radiation study of Hamilton, Rouse and McCutcheon (1972) found that the average longwave flux in the industrialized section of the city exceeded that of the unpolluted control site by as much as 33%. This excess of incoming longwave radiation in the industrial zone occurred between sunrise and sunset and tended to reach a peak at low zenith angles. Another feature of their data was that there was little difference between the control and industrial sites in the night-time incoming longwave flux.

A third feature was that the increased attenuation of sunlight in the industrial atmosphere was almost perfectly matched in terms of energy magnitude by the increase in the longwave radiation from the atmosphere to the surface.

CHAPTER III

SITES, INSTRUMENTS AND METHODS

1. Sites

A. General Description and Features of the Hamilton Area

The measurements for this study were taken at Hamilton, Ontario and in the surrounding rural countryside. The general location is shown in Fig. 1.

With a population of 300,000, Hamilton is one of Canada's major industrial cities and is the main centre for the basic steel-making industry. It occupies a central location in the highly urbanized, heavily populated region located around the western end of Lake Ontario.

The south side of Hamilton Harbour is occupied mainly by primary and secondary steel manufacturing plants. Such a density of heavy industry leads to a very concentrated source of industrial pollutants.

The likely contaminates in Hamilton's atmosphere may be broadly divided into two categories : gases and particulate matter. Included among the gases are carbon monoxide, hydrocarbons, the oxides of nitrogen, and sulphur compounds.

Carbon monoxide is produced during the incomplete combustion of carbonaceous materials, such as would be experienced in coke ovens and blast furnaces. It is a colourless, odorless, and lethal gas.

Hydrocarbons in the urban industrial atmosphere originate in

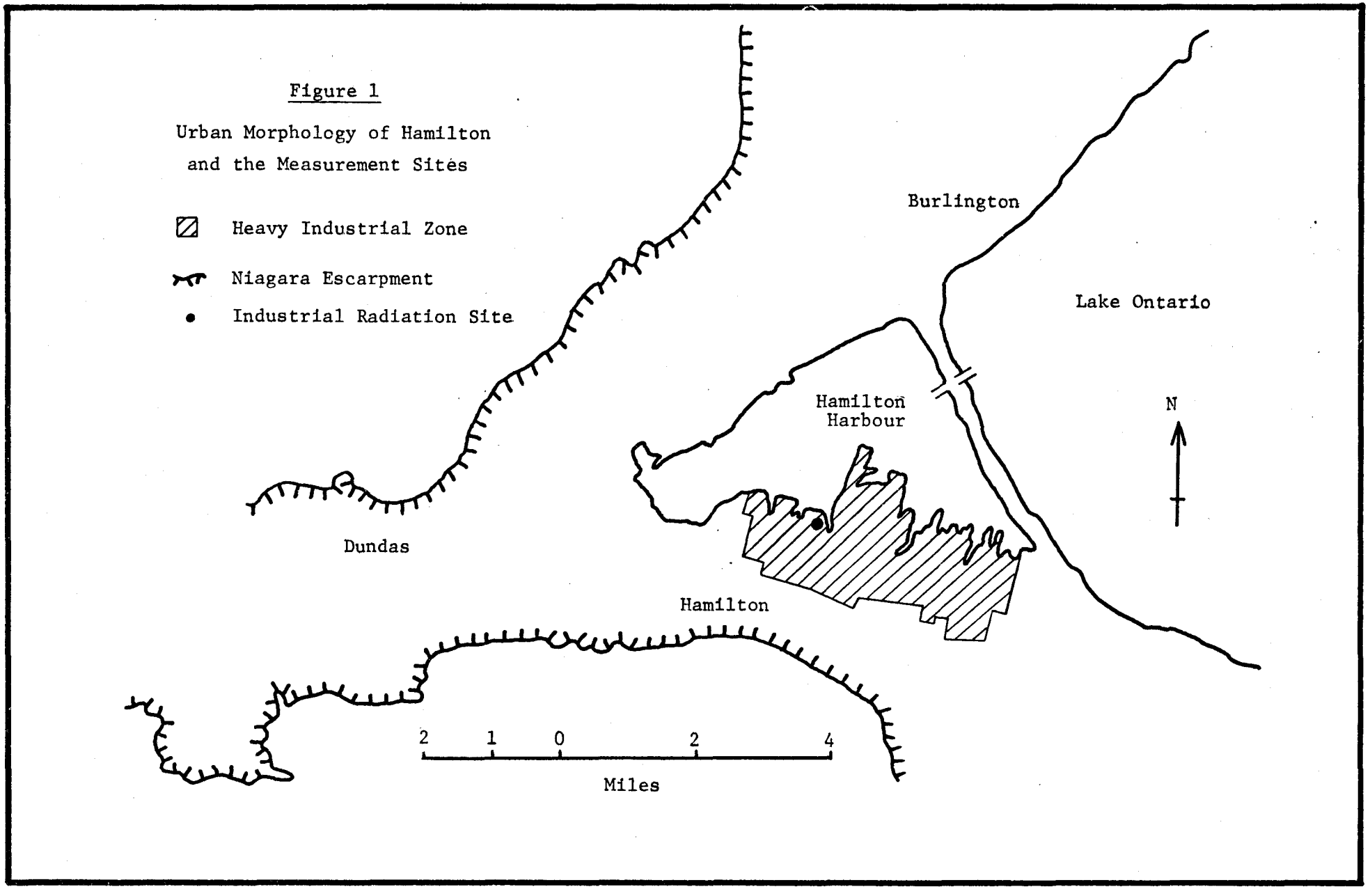
Figure 1
Urban Morphology of Hamilton
and the Measurement Sites
Heavy Industrial Zone
Niagara Escarpment
Industrial Radiation Site
Burlington
Lake Ontario
Hamilton
Harbour
N
Dundas
Hamilton
2 1 0 2 4
Miles

three ways : from the combustion of gasoline, coal, oil, natural gas and wood; from the evaporation of gasoline and industrial solvents; and as a waste byproduct from chemical plants.

Nitrous oxide, nitric oxide, and nitrogen dioxide are produced during high temperature, high pressure combustion processes used in heavy industry, as well as in industrial chemical plants. Nitric oxide is short-lived and turns into the pungent, yellow-brown, and harmful NO_2 gas when exposed to the air.

Since sulphur is an impurity of coal and fuel oil, it enters the air during combustion processes in the form of sulphur dioxide, hydrogen sulphide, sulphurous acid, sulphuric acid, sulphur trioxide, and various sulphates. These are all most likely to be found in Hamilton's atmosphere due to the nature of the industrial activity in the city.

Particulate matter consists of solid and liquid particles, the size range of which varies from greater than 100 μm ($^1/_{10}$ mm) to less than 0.1 μm ($^1/_{10,000}$ mm). Dust, coarse dirt, and fly ash are generally larger than 10 μm and settle out of the air quickly. Particles which are smaller than 10 μm are able to remain much longer as suspended matter in the atmosphere.

Particles below 5 μm in size are known as smoke and fume. Those under 1 μm are called aerosols.

B. Measurement Sites Used in This Project

Radiation measurements were made at two sites. The first, which is called the industrial site, was a rooftop site located immediately

to the west of the largest basic steel producing plant in Canada. The second, termed the control site, was a rooftop site at Mt. Hope Airport, which is situated 7.5 miles south of the industrial site. The control site did not normally exhibit visible atmospheric pollution. Both the industrial and control sites were comparable in terms of height above ground, nature of the surface, absence of local combustion heat, and unlimited sky exposure.

Vertical air temperature profiles were measured over the industrial site and appropriate unpolluted rural sites (depending on wind direction) from about 1000 ft. up to 9500 ft. above the ground.

2. Instrumentation

All of the radiation measurements were made with C.S.I.R.O. radiometers (Swissteco S-1). These instruments employ a thermopile transducer for the sensing element and the top and bottom surfaces can be covered with a variety of transparent or opaque hemispheric domes to allow the measurement of any component radiation flux.

In this experiment, the global radiation (Q+q) was monitored with a pyranometer which used a glass dome over the top surface and a black body cavity over the bottom surface. Thus the solar wavelengths between 0.3 and 3.0 μm were measured. Incoming all-wave radiation (Q+q) + L_i was measured using the second sensor as a pyrradiometer with a polyethylene dome and black body cavity, instead of a glass dome. L_i was derived as the difference between the measurement of the pyranometer and the pyrradiometer.

The temperature of the black body cavity fitted to the pyrradiometer

was measured using a single-junction thermocouple inserted into the cavity wall and referenced to an ice-water bath.

A pyranometer and pyrradiometer were mounted at the industrial site and at the control site. Continuous measurements of the fluxes and the black body cavity temperature were made on strip chart recorders.

Vertical temperature profiles above the city and above the rural countryside were made using a thermopile transducer mounted on the wing strut of a Cessna 172, a high wing monoplane. The sensor was well clear of the propeller slipstream.

Fig. 2 shows the design of the thermopile sensor. The housing consisted of a long aerodynamically smooth inlet nose which faced upwind and an enlarged rear chamber containing the sensor. Under normal aircraft operating speeds the air intake velocity was slowed to 6 m sec^{-1} over the sensor head due to the appropriate increase in cross-sectional area. The plastic housing was covered in aluminum tape which gave effective radiation shielding and was completely blackened inside with spray paint. The thermocouples of the 5-junction thermopile were left bare and radially splayed at the sensor head.

The thermopile circuit was referenced to an ice-water bath in the cockpit. Recording was done on a millivolt strip chart recorder powered from a 12 v battery through a DC/AC inverter.

3. Methods

All measurements were made under cloudless skies, or, in a few cases, under a thin high altitude cirrus or cirrostratus cloud cover. In

Figure 2

Aircraft-Mounted Air Temperature Sensor

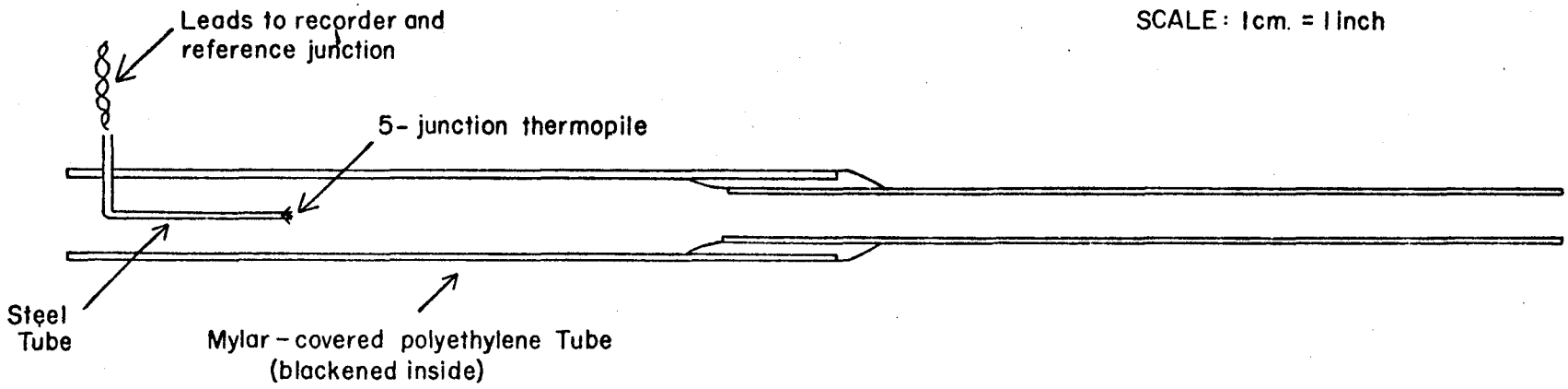

all, data from 10 full or part days between December 22, 1971 and April 28, 1972 were used in this study.

The analysis of the radiation and black body temperature data was done by the planimeter method in order to obtain mean hourly values for each parameter.

The air temperature measurements were made between about 1000 and 9500 ft above the surface. The aircraft was usually operated in tight upward and downward spirals but in the moderate winds which were occasionally encountered aloft it was possible to descend directly by bucking the aircraft in an upwind direction.

CHAPTER IV

RESULTS

The dates on which radiation and the vertical profiles of air temperature were measured are shown in Table 1 along with a description of the visual sky conditions.

The series of daily weather maps in Fig. 3 shows the generalized meteorological conditions which existed on each of the study days.

Data collection was pursued when possible immediately after the passage of a cold front to ensure that clean, dust-free air would be present over the control site. Performing the study under the influence of high pressure, with the ridge of high being over or west of the Hamilton area, ensured that conditions of clear skies and very light winds were maintained.

The presence of clear skies permitted direct comparison of the industrial radiation measurements with the corresponding control site values. Light winds allowed visible concentrations of industrial pollutants to build up into a distinct dome over the city.

1. Radiation Measurements

Hourly totals of $(Q+q)$, L_i, and $(Q+q) + L_i$ at the industrial and control sites, along with the corresponding hourly ratios of industrial/control for $(Q+q)$, L_i, and $(Q+q) + L_i$ are provided in Table 2.

Hourly industrial/control ratios for (Q+q), L_i, and (Q+q) + L_i for each complete 24-hour clear sky study period are plotted in Fig. 4.

Fig. 5 presents the ratios of industrial/control averaged for the entire study period.

All the measurements show that there was significantly greater attenuation of sunlight in the industrial atmosphere than for the control site. The increased attenuation of solar radiation at the industrial site began immediately at sunrise and persisted until sunset. For all measurements the attenuation averaged 12.3%.

The incoming longwave radiation was notably greater at the industrial site than at the control site during the daylight hours. Although this excess of incoming infrared radiation operated between sunrise and sunset it tended to reach a peak around mid-day. When averaged for all daytime measurements the incoming longwave flux reached an excess of about 21%.

There was little difference between sites in the amount of L_i received at night, either for averaged or for individual periods.

Virtually no difference existed between the industrial and control sites in the total incoming radiation either at night or during the day when all measurements were averaged. Individual hourly ind/con ratios when averaged were within 4% of unity, as shown in Fig. 5.

It appears, then, that the decrease in (Q+q) experienced during the daytime in the industrial zone was largely compensated by the corresponding increase in L_i so that the hourly totals of (Q+q) + L_i remained the same for both the industrial and control sites.

TABLE 1

MEASUREMENT DATES AND SKY CONDITIONS

Date	Sky Conditions
December 22, 1971	Clear all day
March 10, 1972	Clear; Cirrostratus cloud by mid-day
March 27	Clear all day
March 28	Clear all day
April 18	Clear all day
April 21	Clear; Cirrostratus cloud by afternoon
April 25	Clear all day
April 26	Clear; Cirrostratus cloud by late morning
April 27	Clear all day
April 28	Clear all day

Figure 3

Daily Weather Maps

(Map time is 0700 EST. Isobar figures are in millibars. Areas of precipitation at map time are shaded. Symbols: H - high, L - low.)

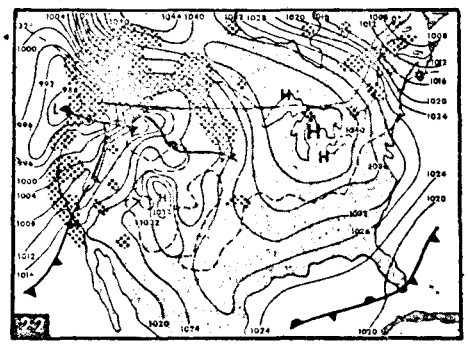

December 22, 1971

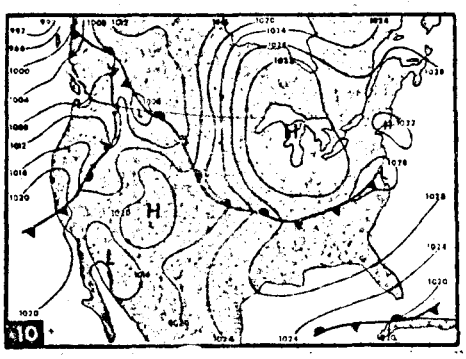

March 10, 1972

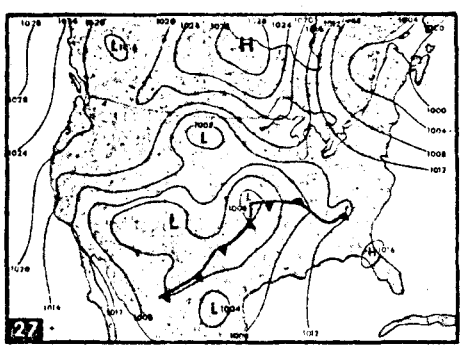

March 27, 1972

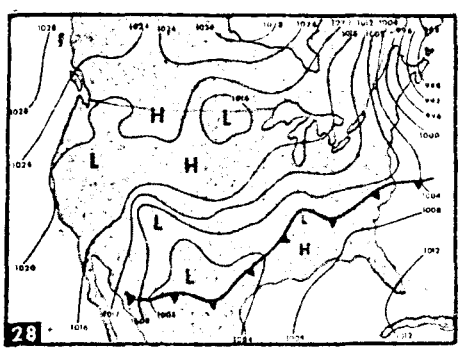

March 28, 1972

Figure 3 (continued)

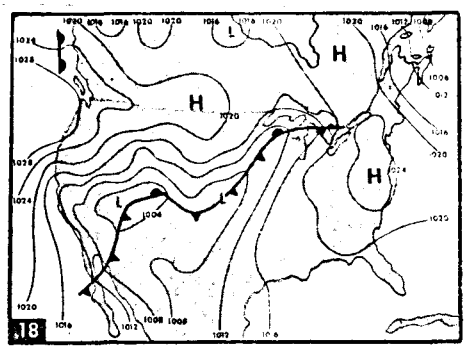

April 18, 1972

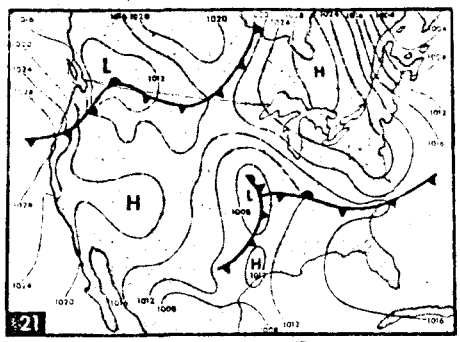

April 21, 1972

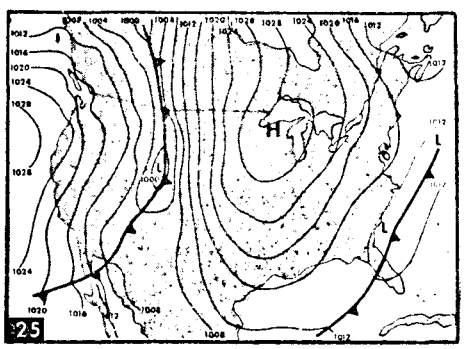

April 25, 1972

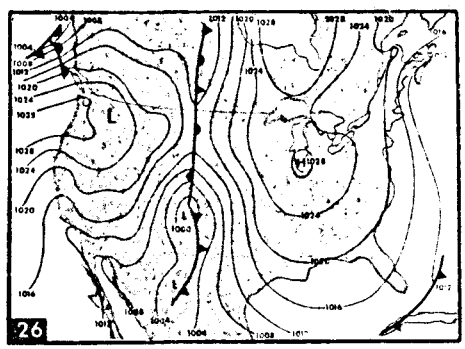

April 26, 1972

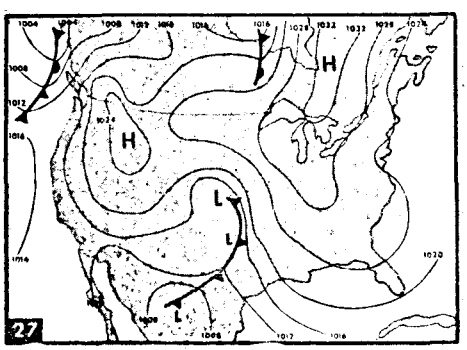

April 27, 1972

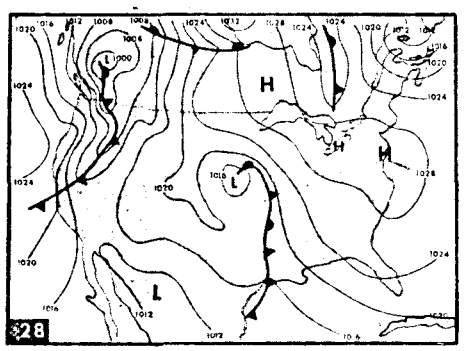

April 28, 1972

TABLE 2

HOURLY TOTALS OF RADIATION MEASUREMENTS AT THE INDUSTRIAL AND CONTROL SITES AND RATIOS OF IND/CON FOR CLEAR SKY PERIODS.
(Radiation values in ly hr^{-1})

Date	Hour Ending	Industrial			Control			Industrial/Control		
		Q+q	L_i	Q+q+L_i	Q+q	L_i	Q+q+L_i	Q+q	L_i	Q+q+L_i*
Dec. 22/ 71	0400	0	13.32		0	13.84			0.96	
	0500	0	13.42		0	13.63			0.98	
	0600	0	13.37		0	13.82			0.97	
	0700	0	13.80		0	14.06			0.98	
	0800	0.53	15.43	15.96	0.68	14.76	15.44	0.78	1.04	1.03
	0900	8.80	16.00	24.80	0.89	13.98	23.87	0.89	1.14	1.04
	1000	18.86	17.77	36.63	20.73	15.52	36.25	0.91	1.14	1.01
	1100	27.57	18.64	46.21	30.30	12.28	45.58	0.91	1.22	1.01
	1200	31.92	21.59	53.51	35.47	16.45	51.92	0.90	1.31	1.03
	1300	30.49	20.17	50.66	35.05	15.80	50.85	0.87	1.27	1.00
	1400	25.17	21.07	46.24	29.96	16.73	46.69	0.84	1.26	0.99
	1500	18.09	21.01	39.10	21.04	16.52	37.56	0.86	1.27	1.04
	1600	7.30	18.25	25.55	9.24	16.90	26.14	0.79	1.08	0.98
	1700	0.30	16.72	17.02	0.55	16.96	17.51	-	0.99	-
	1800	0	16.24		0	15.88			1.02	
	1900	0	16.10		0	16.03			1.00	
	2000	0	15.78		0	15.61			1.01	
	2100	0	15.71		0	15.44			1.02	
	2200	0	16.30		0	15.82			1.03	
Mar. 10/ 72	0200	0	11.93		0	12.02			0.99	
	0300	0	11.67		0	12.16			0.96	
	0400	0	12.20		0	12.06			1.01	
	0500	0	12.16		0	11.81			1.03	
	0600	0	12.17		0	11.90			1.02	
	0700	3.72	12.21	15.93	4.23	12.62	16.85	0.88	0.97	0.95
	0800	17.86	12.43	30.29	19.20	12.53	31.73	0.93	0.99	0.96
	0900	32.79	13.39	46.18	34.88	13.02	47.90	0.94	1.03	0.96
	1000	44.77	16.74	61.51	49.20	12.84	62.04	0.91	1.30	0.99
	1100	54.51	16.11	70.62	58.61	13.66	72.27	0.93	1.18	0.98
	1200	60.49	12.63	73.12	63.67	14.08	77.75	0.95	0.90	0.94

* Night-time values of this ratio appear in the Ind/Con L_i column

Date	Hour Ending	Industrial			Control			Industrial/Control		
		Q+Q	L_i	Q+q+L_i	Q+q	L_i	Q+q+L_i	Q+q	L_i	Q+q+L_i
Mar. 27	0100	0	15.58		0	16.20			0.96	
	0200	0	14.78		0	15.83			0.93	
	0300	0	14.10		0	14.96			0 94	
	0400	0	14.29		0	14.72			0.97	
	0500	0	14.67		0	14.78			0.99	
	0600	0.21	16.51	16.72	0.32	16.24	16.56		1.02	
	0700	7.41	17.66	25.07	10.15	15.38	25.53	0.73	1.15	0.98
	0800	20.50	21.73	42.23	25.95	15.66	41.61	0.79	1.39	1.01
	0900	35.00	26.05	61.05	43.21	16.07	59.28	0.81	1.62	1.03
	1000	47.64	27.34	74.98	56.05	16.86	72.91	0.85	1.62	1.03
	1100	59.62	23.97	83.59	65.63	17.39	83.02	0.91	1.38	1.01
	1200	67.28	22.28	89.56	70.12	17.54	87.66	0.96	1.27	1.02
	1300	61.89	29.13	91.02	68.04	17.71	85.75	0.91	1.64	1.06
	1400	58.48	28.01	86.49	64.98	18.04	83.02	0.90	1.55	1.04
	1500	46.29	29.69	75.98	52.06	17.58	69.64	0.89	1.69	1.09
	1600	36.77	26.97	63.74	42.75	17.88	60.63	0.86	1.51	1.05
	1700	21.16	24.10	45.26	25.80	18.13	43.93	0.82	1.32	1.03
	1800	7.11	20.57	27.68	8.89	17.80	26.69	0.80	1.13	1.04
	1900	0.41	17.82	18.23	0.54	17.46	18.00	0.76	1.02	1.01
	2000	0	16.04		0	15.97			1.00	
	2100	0	16.51		0	16.32			1.01	
	2200	0	16.26		0	16.06			1.01	
	2300	0	16.80		0	16.71			1.01	
	2400	0	16.71		0	16.53			1.02	
Mar. 28	0100	0	16.34		0	16.28			1.00	
	0200	0	15.81		0	15.99			0.99	
	0300	0	16.29		0	16.82			0.97	
	0400	0	15.26		0	15.43			0.99	
	0500	0	15.60		0	15.47			1.01	
	0600	0.18	15.51	15.69	0.28	15.79	16.07		0.97	
	0700	8.52	16.66	25.18	10.52	16.60	27.12	0.81	1.00	0.93
	0800	24.50	18.40	42.90	28.16	16.58	44.74	0.87	1.11	0.96
	0900	38.28	21.18	59.46	43.50	17.74	61.24	0.88	1.19	0.97
	1000	53.19	19.72	72.91	57.81	17.87	75.68	0.92	1.10	0.96
	1100	62.36	21.59	83.94	67.05	17.47	84.52	0.93	1.23	0.99
	1200	64.66	23.77	88.43	71.84	18.28	90.12	0.90	1.30	0.98
	1300	65.60	23.51	89.11	72.09	18.53	90.62	0.91	1.27	0.98
	1400	54.76	32.39	86.15	66.78	19.29	86.07	0.82	1.67	1.00
	1500	48.14	27.87	76.01	56.63	18.01	74.64	0.85	1.55	1.02
	1600	38.44	23.82	62.26	42.24	19.10	61.34	0.91	1.25	1.02
	1700	24.64	24.27	48.91	26.78	18.88	45.66	0.92	1.28	1.07
	1800	8.34	29.19	28.53	9.27	19.16	28.43	0.90	1.05	1.00
	1900	0.27	18.25	18.52	0.31	17.66	17.97	0.86	1.03	1.03
	2000	0	18.68		0	18.53			1.01	

Date	Hour Ending	Industrial			Control			Industrial/Control		
		Q+q	L_i	Q+q+L_i	Q+q	L_i	Q+q+L_i	Q+q	L_i	Q+q+L_i
Mar.	2100	0	16.98		0	17.15				
28	2200	0	17.01		0	17.03				
	2300	0	17.59		0	17.62				
	2400	0	18.54		0	18.06				
Apr.	0100	0	20.74		0	19.98				
18	0200	0	20.41		0	19.47				
	0300	0	21.06		0	19.68				
	0400	0	20.28		0	19.10				
	0500	0	20.38		0	19.23				
	0600	2.52	21.22	23.74	3.32	20.23	23.55	0.76	0.76	1.01
	0700	14.01	25.87	39.88	17.96	21.07	39.03	0.78	0.78	1.02
	0800	29.84	25.51	55.35	35.10	20.85	55.95	0.85	0.85	0.99
	0900	46.20	24.81	71.01	50.22	21.43	71.65	0.92	0.92	0.99
	1000	43.09	31.55	85.64	62.90	23.47	86.37	0.86	0.86	0.99
	1100	62.54	36.52	99.06	71.88	24.02	95.90	0.87	0.87	1.03
	1200	69.35	32.83	102.18	77.06	24.67	101.73	0.90	0.90	1.00
	1300	68.40	34.67	103.07	76.85	25.92	102.77	0.89	0.89	1.01
	1400	65.15	34.82	99.97	70.82	26.36	97.18	0.92	0.92	1.03
	1500	57.64	36.68	94.32	61.98	28.56	90.54	0.93	0.93	1.04
	1600	44.70	35.58	80.28	49.12	28.80	77.92	0.91	0.91	1.03
	1700	26.32	32.37	58.69	28.30	27.15	55.45	0.93	0.93	1.06
	1800	13.38	30.83	44.21	15.20	26.86	42.06	0.88	0.88	1.05
	1900	1.91		31.29	2.46	26.13	28.59	0.78	1.12	1.09
	2000	0			0	24.89			1.04	
	2100	0			0	24.71			1.02	
	2200	0			0	23.91			1.00	
	2300	0			0	24.46			1.00	
	2400	0			0	23.90			1.00	
Apr.	0400	0			0	19.12			1.00	
21	0500	0			0	19.59			1.02	
	0600	1.98		24.12	3.83	20.47	24.30		1.08	
	0700	16.21		40.47	18.21	21.39	39.60	0.89	1.13	1.02
	0800	33.45		57.52	35.97	21.76	57.73	0.93	1.11	1.00
	0900	43.02		67.13	51.06	21.15	72.21	0.86	1.14	0.93
	1000	56.21		81.18	63.88	22.60	86.48	0.88	1.10	0.94
	1100	63.54		92.47	73.96	22.47	96.43	0.86	1.28	0.96
	1200	71.38		96.62	78.43	23.31	101.74	0.91	1.08	0.95
	1300	71.51		98.04	76.82	23.12	99.94	0.93	1.15	0.98
	1400	58.79		88.43	65.40	24.96	90.36	0.90	1.19	0.98

Date	Hour Ending	Industrial			Control			Industrial/Control		
		Q+q	L_i	Q+q+L_i	Q+q	L_i	Q+q+L_i	Q+q	L_i	Q+q+L_i
Apr.	0100	0	18.65		0	19.85			0.94	
25	0200	0	18.07		0	19.04			0.95	
	0300	0	19.03		0	19.39			0.98	
	0400	0	18.26		0	18.81			0.97	
	0500	0	18.62		0	18.96			0.98	
	0600	3.03	21.73	24.76	3.89	19.17	23.06	0.78	1.13	1.07
	0700	16.93	24.73	41.66	20.16	19.82	39.98	0.84	1.25	1.04
	0800	34.23	26.30	60.53	38.45	19.54	57.99	0.89	1.34	1.04
	0900	49.09	24.61	73.70	52.76	19.38	72.14	0.93	1.27	1.02
	1000	59.81	25.21	85.02	65.02	19.71	84.73	0.92	1.28	1.01
	1100	65.26	29.52	94.78	74.14	20.77	94.91	0.88	1.42	1.00
	1200	73.61	26.96	100.57	79.12	20.53	99.65	0.93	1.31	1.01
	1300	74.06	26.61	100.67	78.87	20.89	99.76	0.94	1.27	1.01
	1400	67.59	25.73	93.32	74.42	21.68	96.10	0.91	1.19	0.97
	1500	58.78	25.89	84.67	64.55	21.81	86.36	0.91	1.19	0.98
	1600	47.11	23.89	71.09	52.35	22.29	74.64	0.90	1.06	0.95
	1700	33.14	28.96	62.10	37.39	22.68	60.07	0.89	1.28	1.03
	1800	16.40	27.06	43.46	19.07	21.83	40.90	0.86	1.24	1.06
	1900	3.13	24.05	25.18	3.77	22.01	25 78	0.83	1.09	0.98
	2000	0	21.78		0	20.98			1.04	
	2100	0	21.49		0	21.38			1.01	
	2200	0	20.83		0	20.81			1.00	
	2300	0	20.82		0	20.86			1.00	
	2400	0	20.21		0	20.09			1.01	
Apr.	0100	0	19.75		0	19.70			1.00	
26	0200	0	19.78		0	20.21			0.98	
	0300	0	19.32		0	19.49			0.99	
	0400	0	18.49		0	18.68			0.99	
	0500	0.12	16.69	16.81	0.18	17.80	17.98	0.86	0.94	
	0600	2.88	17.16	20.04	3.35	18.38	21.73	0.93	0.93	0.93
	0700	15.86	19.52	35.38	17.05	19.53	36.58	0.91	1.00	0.97
	0800	32.14	23.89	55.03	35.32	19.89	55.21	0.94	1.20	1.00
	0900	48.71	24.61	73.32	51.82	20.81	72.63	0.93	1.18	1.01
	1000	58.28	25.83	84.11	62.67	20.62	83.29	0.97	1.25	1.01
	1100	70.87	25.87	96.74	73.06	21.68	94.74	0.98	1.19	1.02
	1200	77.57	23.32	100.89	79.15	22.01	101.16		1.06	1.00
Apr.	0100	0	18.81		0	19.01			0.99	
27	0200	0	18.74		0	18.53			1.01	
	0300	0	18.93		0	18.70			1.01	
	0400	0	18.68		0	18.13			1.03	
	0500	0.12	19.05	19.17	0.24	18.85	19.09		1.02	
	0600	3.57	21.66	25.23	4.70	19.81	24.51	0.76	1.09	1.03
	0700	15.99	25.15	41.14	20.50	19.18	39.68	0.78	1.31	1.04

Date	Hour Ending	Industrial			Control			Industrial/Control		
		Q+q	L_i	Q+q+L_i	Q+q	L_i	Q+q+L_i	Q+q	L_i	Q+q+L_i
Apr. 27	0800	32.94	24.28	57.22	37.03	19.60	56.63	0.89	1.24	1.01
	0900	47.61	25.10	72.71	52.43	20.50	72.93	0.91	1.22	1.00
	1000	59.62	26.91	86.53	64.85	20.77	85.62	0.92	1.30	1.01
	1100	70.10	27.46	97.56	74.46	21.38	95.84	0.94	1.28	1.02
	1200	72.94	31.24	104.18	79.32	22.03	101.35	0.92	1.42	1.03
	1300	69.58	-	-	79.21	22.38	101.59	0.88	-	-
	1400	65.92	30.97	96.89	73.96	23.14	97.10	0.89	1.34	1.00
	1500	59.19	31.22	90.41	65.02	22.86	87.88	0.91	1.37	1.03
	1600	46.59	32.79	79.38	51.76	23.80	75.56	0.90	1.38	1.05
	1700	32.90	30.19	63.09	36.48	21.98	58.46	0.90	1.37	1.08
	1800	16.27	23.44	39.71	18.92	21.68	40.60	0.86	1.08	0.98
	1900	3.81	22.58	26.39	4.89	20.42	25.31	0.78	1.11	1.04
	2000	0.25	20.13	20.38	0.36	20.13	20.49	-	1.00	-
	2100	0	20.82		0	20.87			1.00	
	2200	0	20.70		0	20.49			1.01	
	2300	0	21.26		0	20.63			1.03	
	2400	0	20.53		0	19.90			1.03	
Apr. 28	0100	0	19.66		0	19.07			1.03	
	0200	0	19.85		0	19.62			1.01	
	0300	0	19.34		0	19.54			0.99	
	0400	0	18.50		0	18.89			0.98	
	0500	0.16	17.63	17.79	0.21	18.92	19.13	0.76	0.93	0.93
	0600	3.23	19.53	22.76	4.20	19.59	23.79	0.77	1.00	0.96
	0700	12.44	22.02	34.46	15.36	20.15	35.51	0.81	1.09	0.97
	0800	18.90	21.93	40.83	23.92	20.91	44.83	0.79	1.05	0.91
	0900	37.58	25.21	62.79	46.40	21.32	67.72	0.81	1.18	0.93
	1000	51.08	27.83	77.91	56.55	22.15	78.70	0.90	1.26	0.99
	1100	61.94	27.96	89.90	69.04	22.18	91.22	0.90	1.26	0.99
	1200	69.49	30.68	100.17	74.48	23.30	97.78	0.93	1.32	1.02
	1300	69.61	30.27	99.88	77.36	24.87	102.23	0.90	1.22	0.98
	1400	65.06	31.58	96.64	71.42	24.18	95.60	0.91	1.31	1.01
	1500	59.28	31.25	90.53	65.00	24.76	89.76	0.91	1.26	1.01
	1600	45.97	27.65	73.62	50.52	26.07	76.59	0.91	1.06	0.96
	1700	30.27	25.16	55.46	34.40	24.88	59.28	0.88	1.01	0.94
	1800	16.17	25.85	41.02	18.80	24.14	42.94	0.86	1.07	0.96
	1900	3.31	23.75	27.06	4.14	23.58	27.72	0.80	1.01	0.98
	2000	0.24	22.17	22.41	0.36	22.03	22.39	-	1.00	-
	2100	0	20.65		0	20.43			1.01	
	2200	0	20.56		0	20.58			1.00	
	2300	0	20.38		0	20.60			0.99	
	2400	0	21.35		0	21.84			0.98	

Figure 4a

Hourly Ind/Con Ratios for March 27

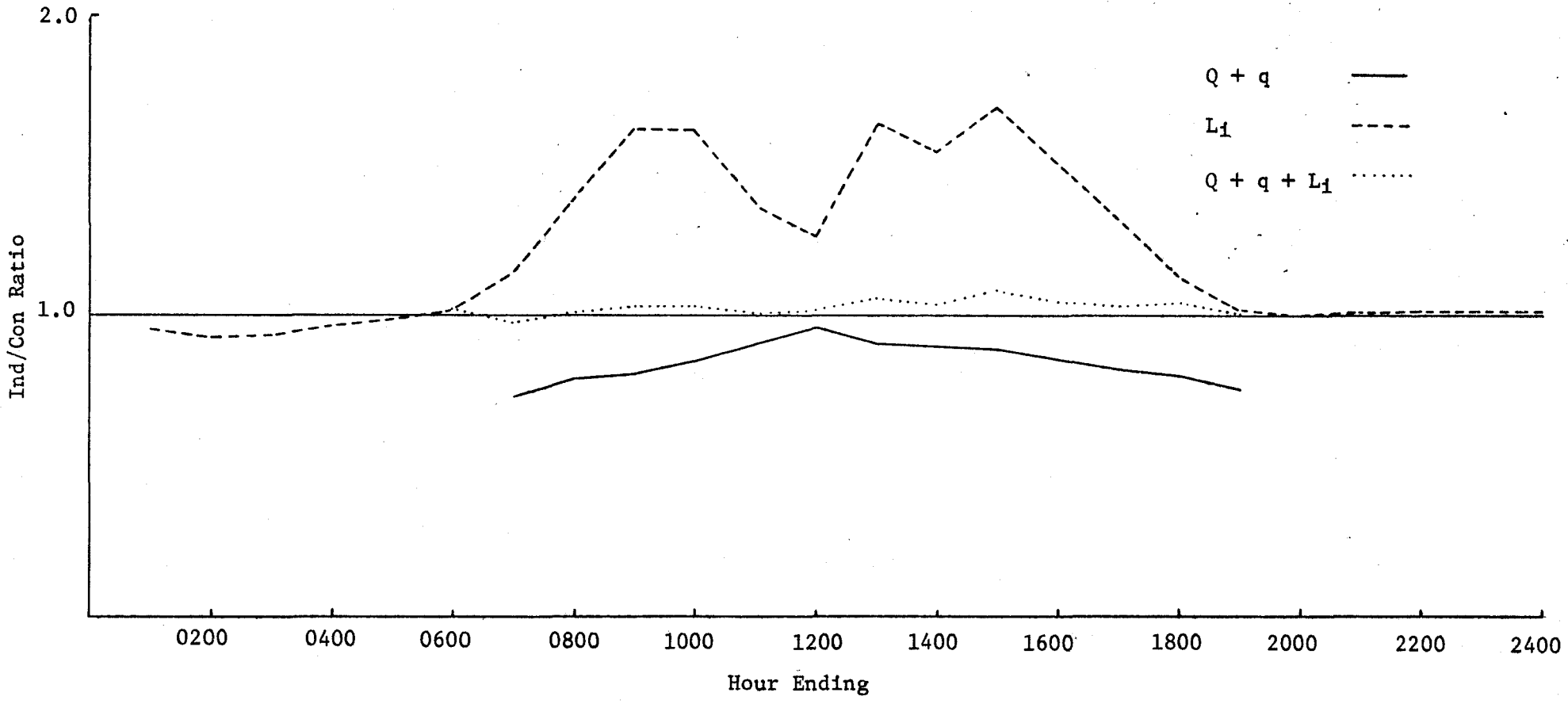

Figure 4b

Hourly Ind/Con Ratios for March 28

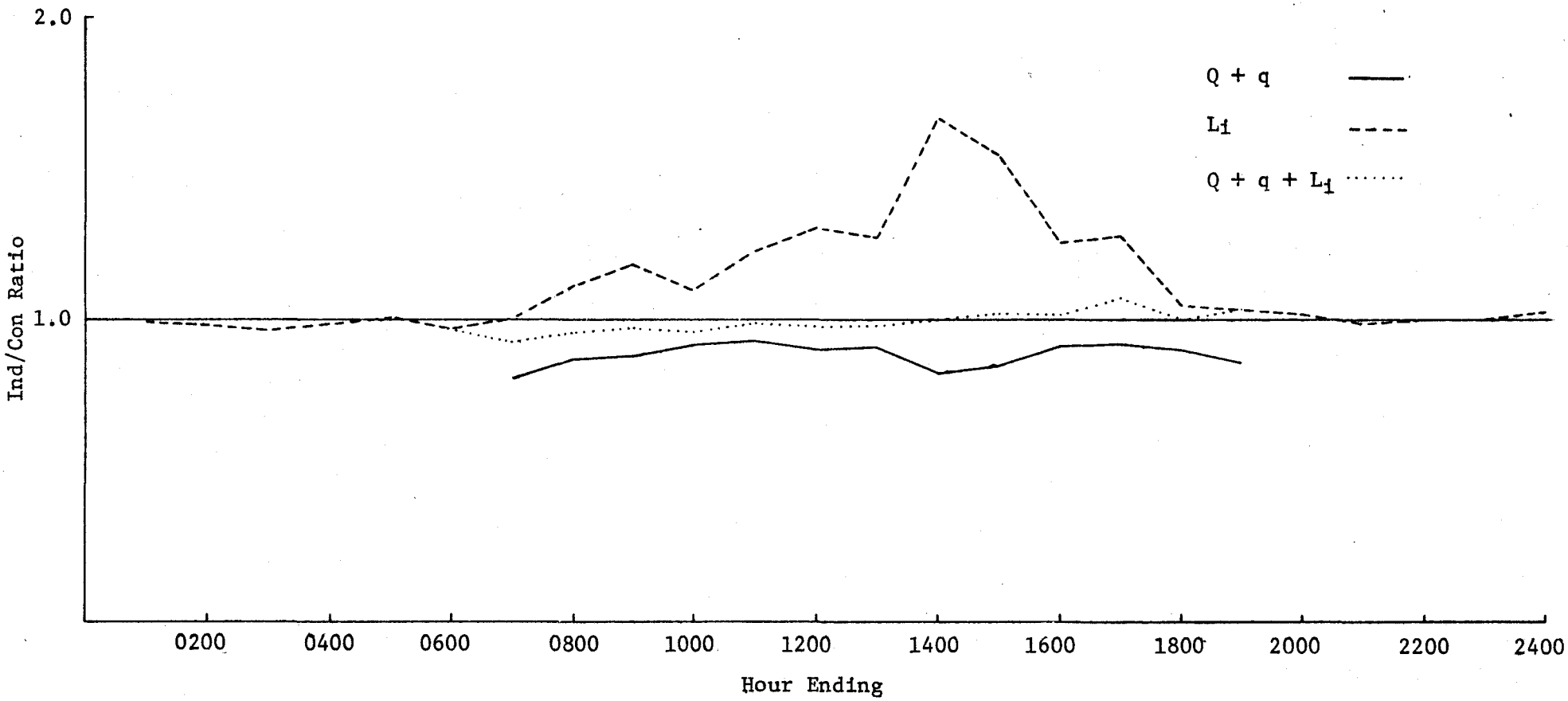

Figure 4c

Hourly Ind/Con Ratios for April 18

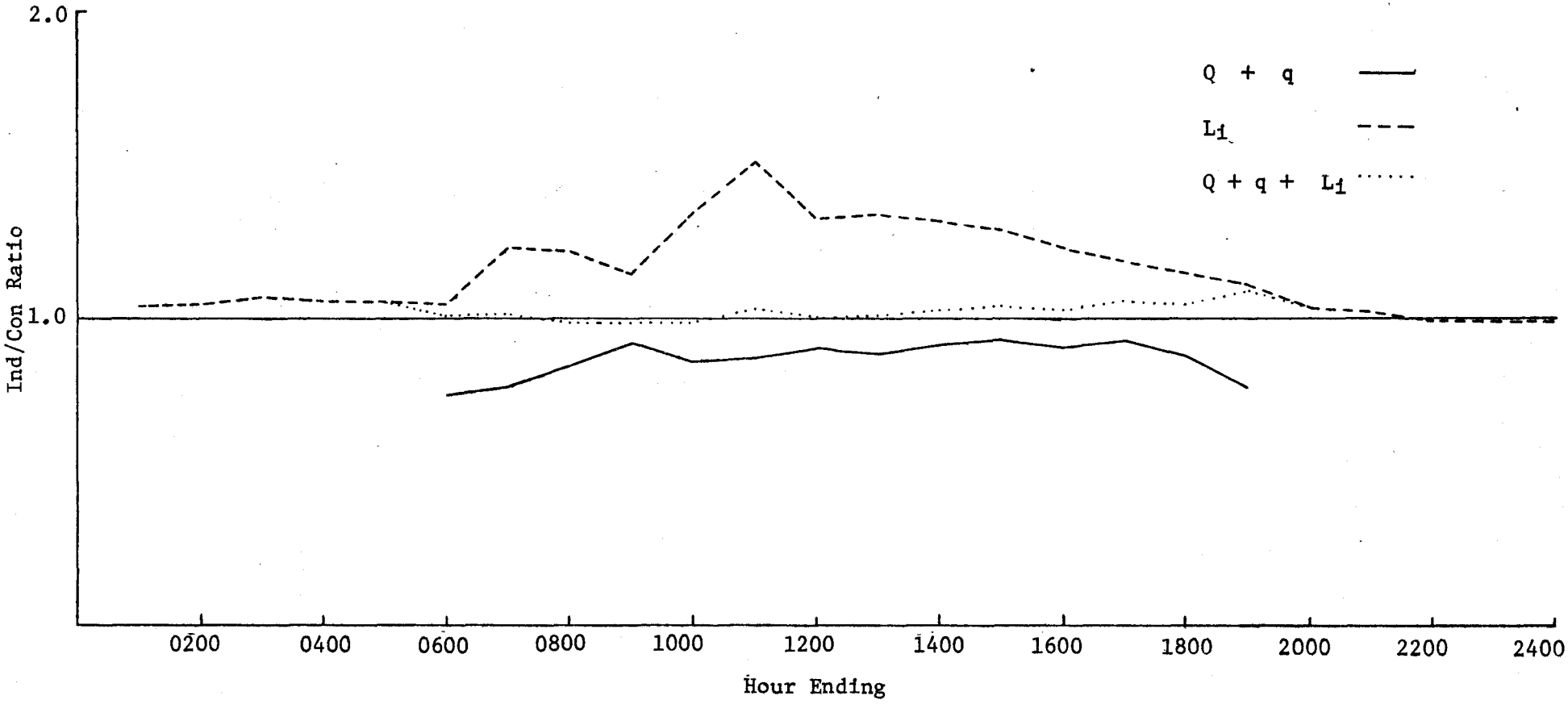

Figure 4d

Hourly Ind/Con Ratios for April 25

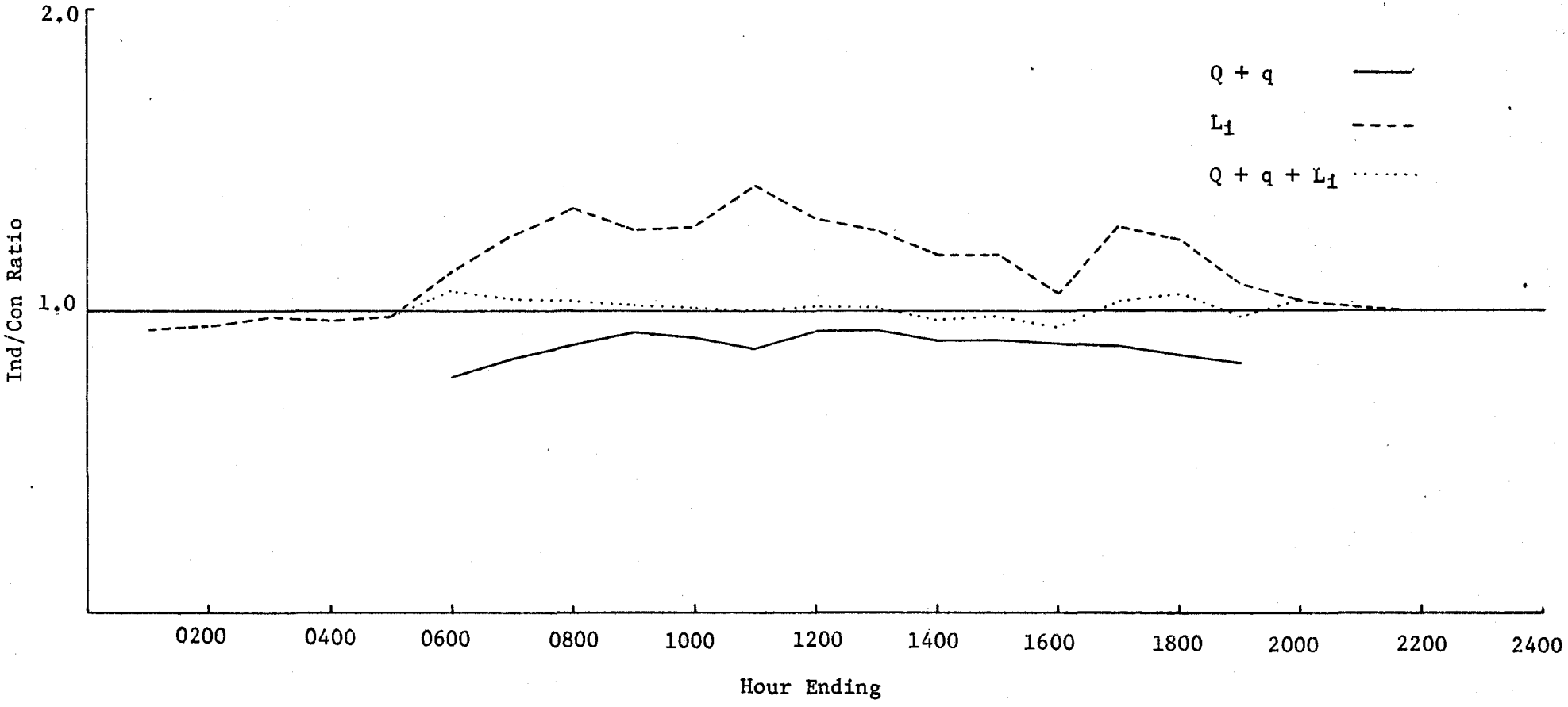

Figure 4e

Hourly Ind/Con Ratios for April 27

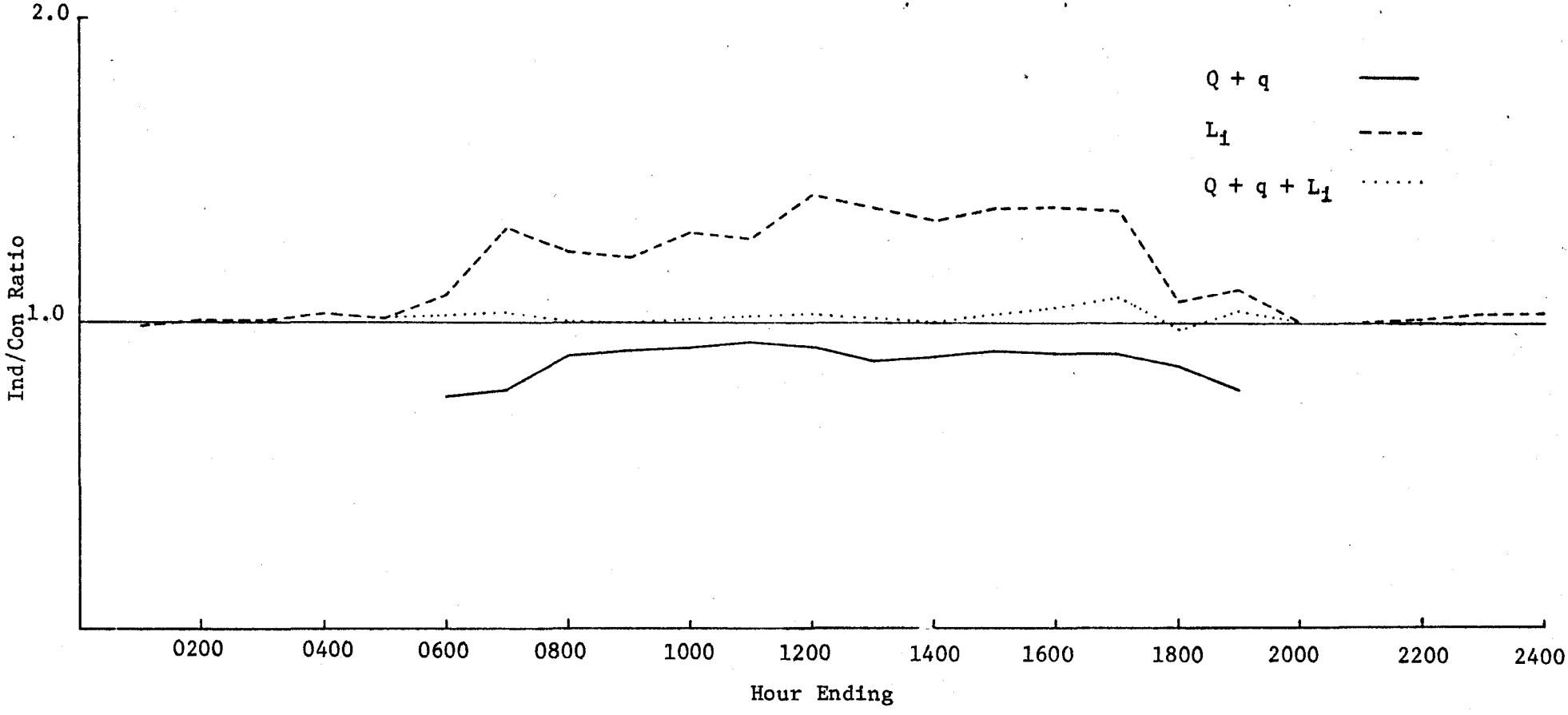

Figure 4f

Hourly Ind/Con Ratios for April 28

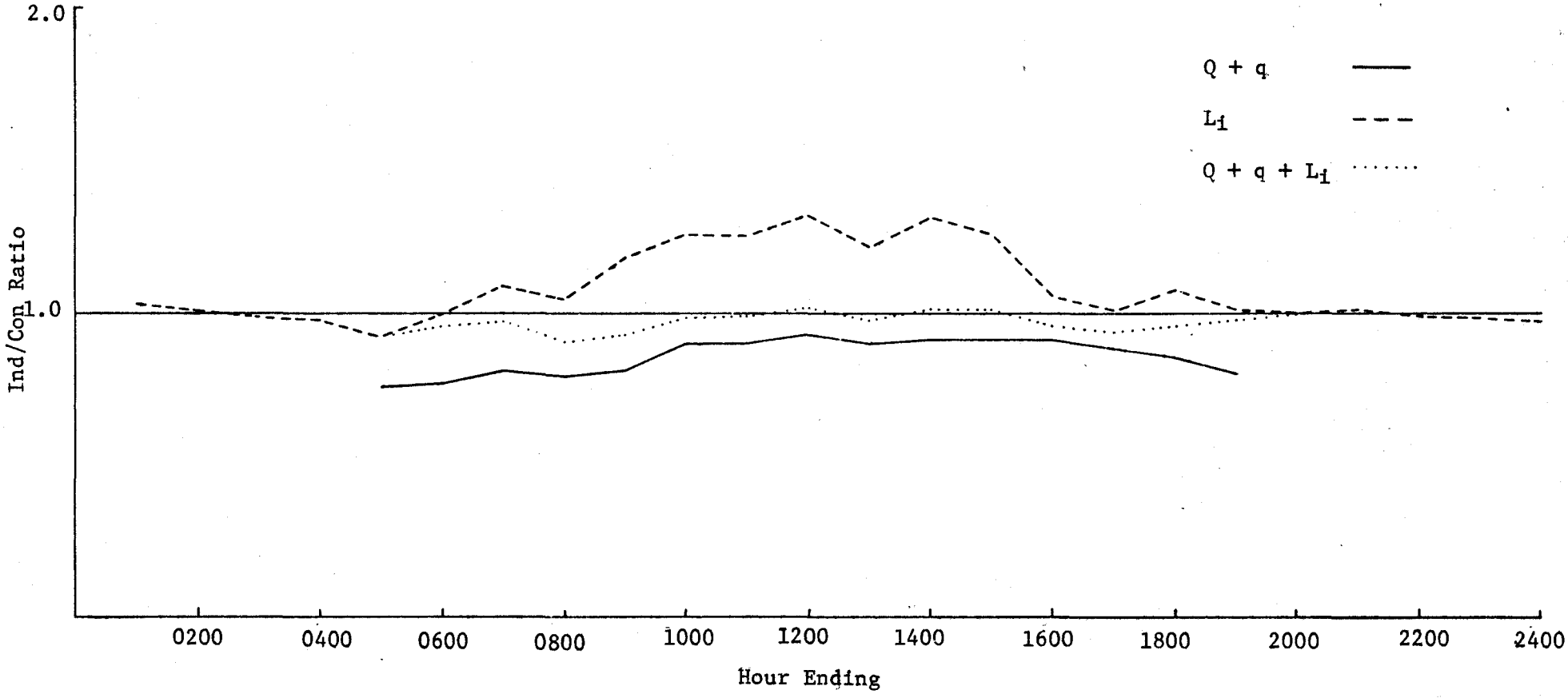

Figure 5

Hourly Ind/Con Ratios Averaged for All Data Periods

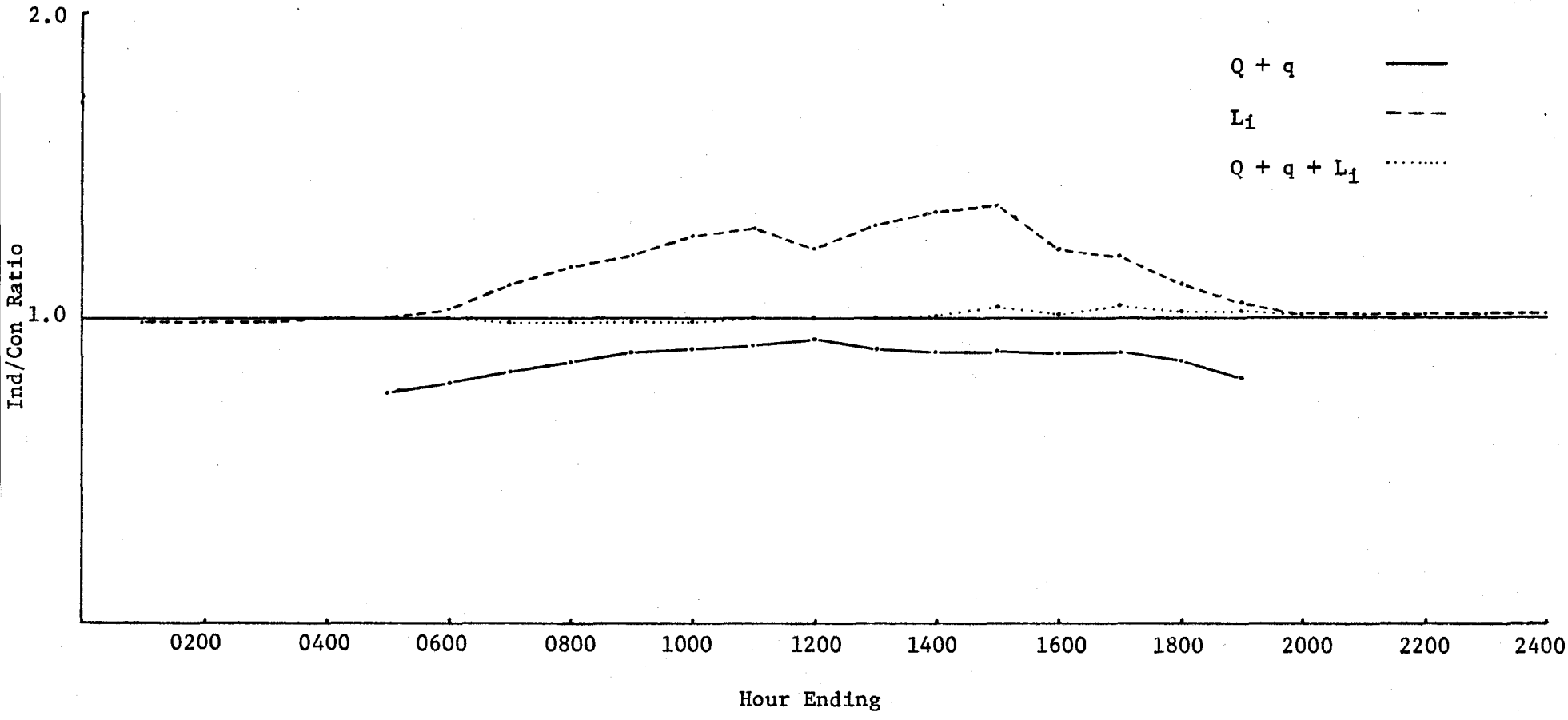

2. Vertical Temperature Profiles

Vertical air temperature profiles measured over the industrial and control sites are plotted in Fig. 6.

There are a number of features to be noted when comparing the profiles over the industrial site to those above the control site. The industrial profiles consistently exhibit a marked elevated temperature inversion during nighttime hours. This inversion diminishes in magnitude as the sunlight becomes more intense but increases again toward sunset. It reaches a minimum about two hours after solar noon.

Another feature of the elevated temperature inversion is that its height increases to a maximum about two hours after solar noon and descends again beyond this point in time. This is shown in Table 3. For all measurement days, the average rate of change in height was ± 168 ft. $hour^{-1}$; the maximum rate of change in height was -300 ft $hour^{-1}$ and this occurred on the afternoon of March 10, 1972.

The rates of temperature change below the inversion level at various heights above the industrial and control sites are shown in Table 4. The rates of temperature change at any height above the industrial area nearly always exceed those measured over the control site at the same height. The average rates for individual heights during the morning and afternoon periods over the industrial and control sites are given in Table 5.

Figure 6

Vertical Temperature Profiles in the Industrial and Control Atmospheres

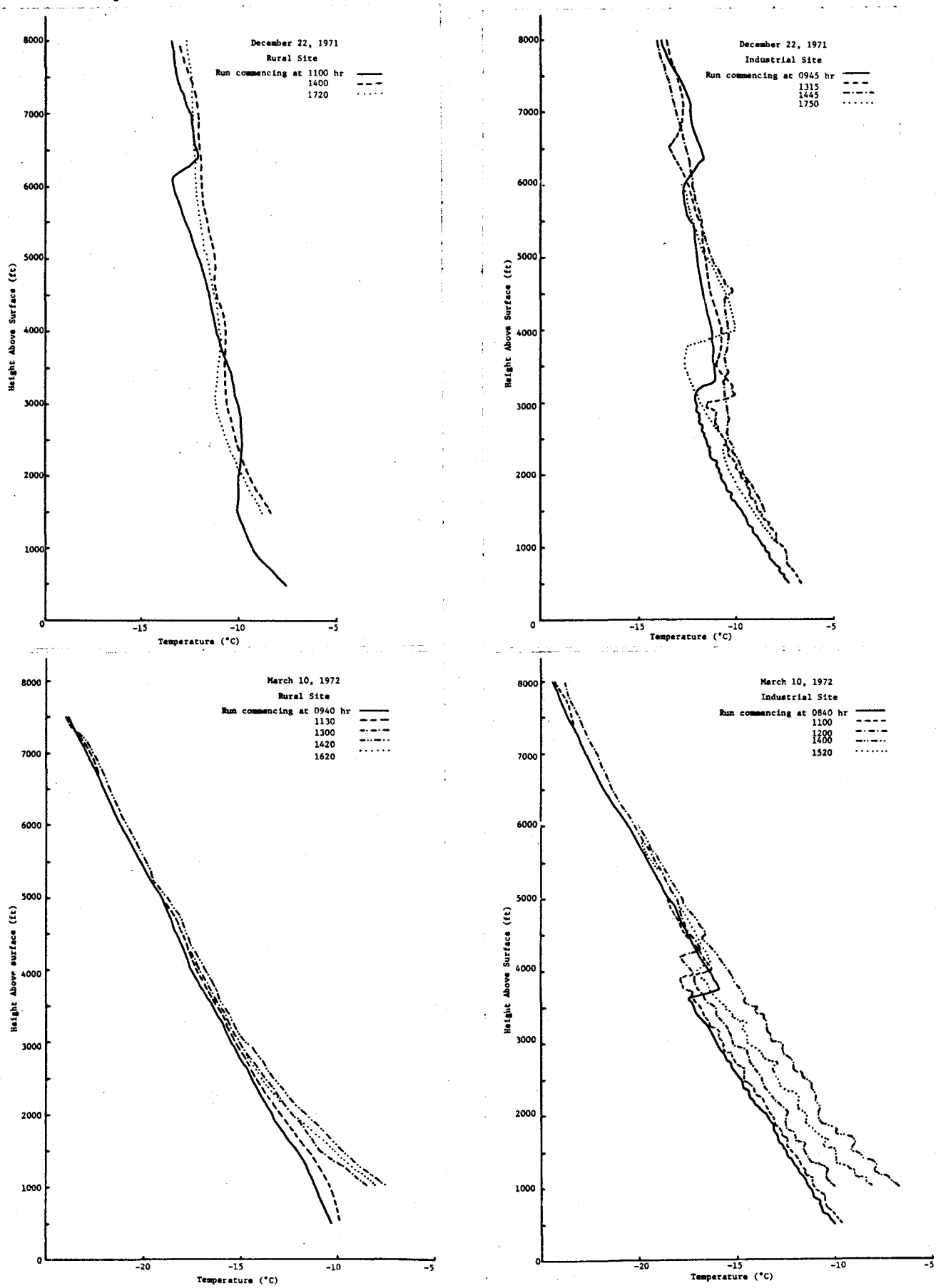

Figure 6 (continued)

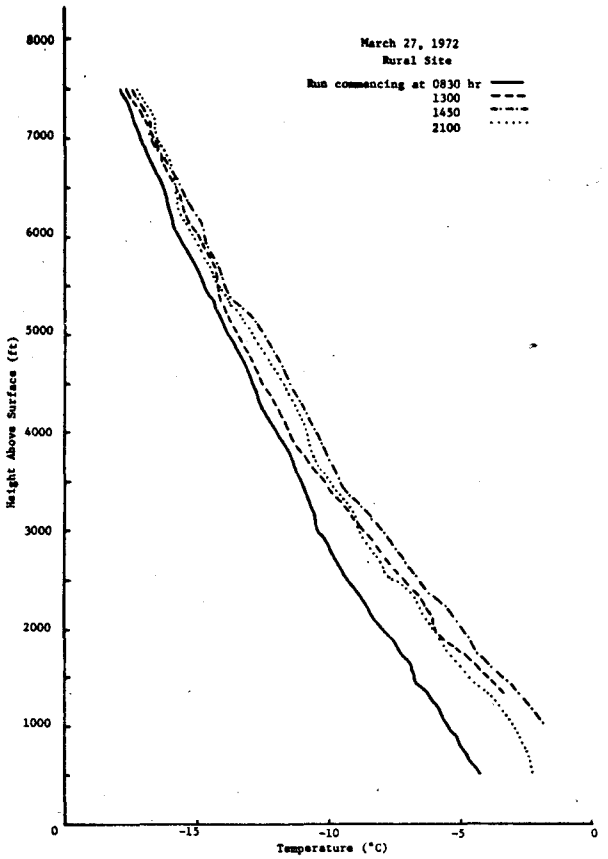

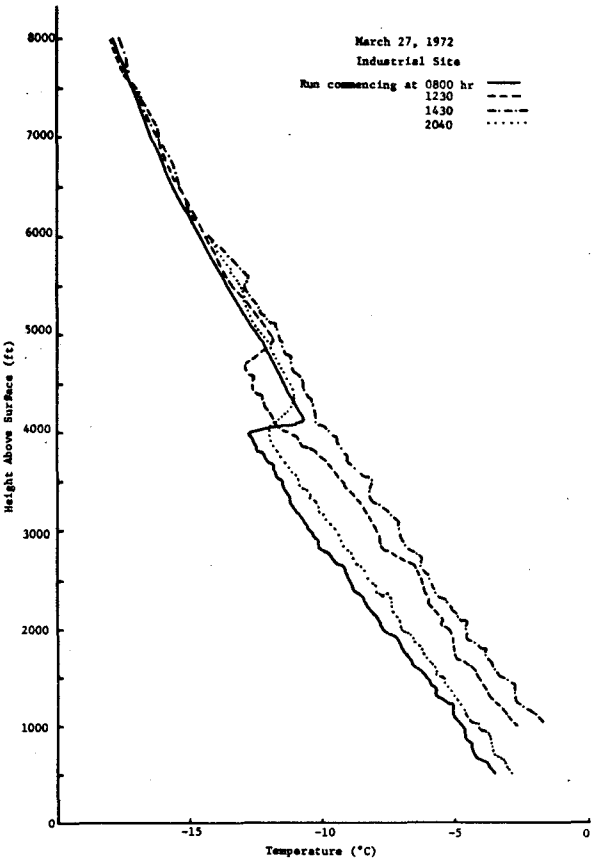

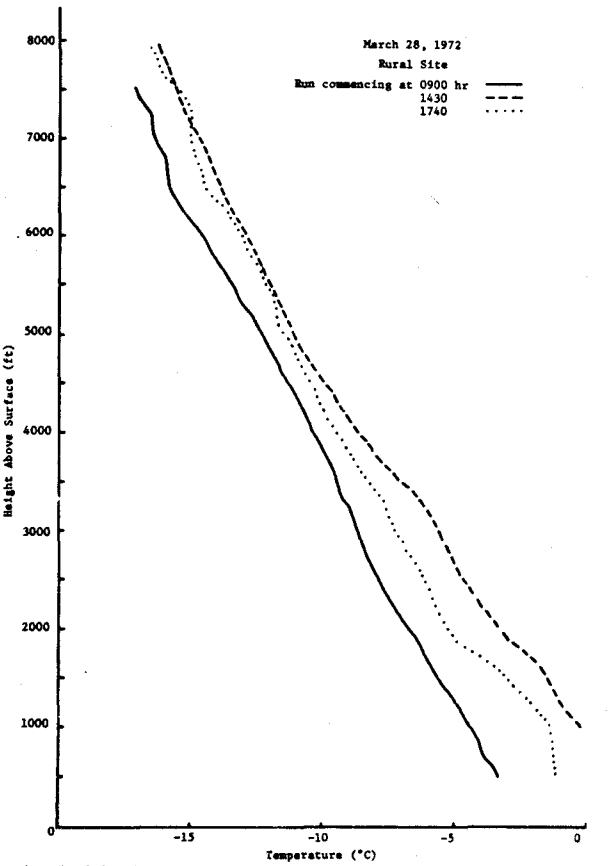

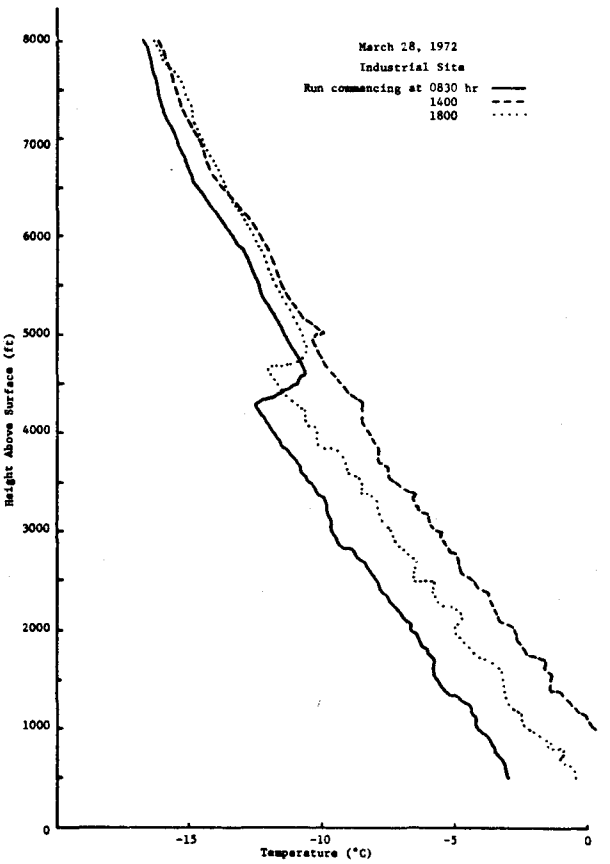

Figure 6 (continued)

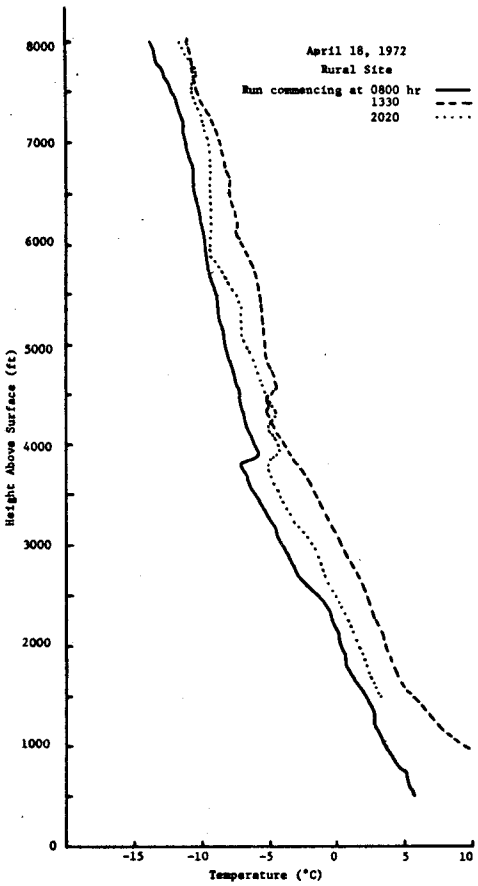

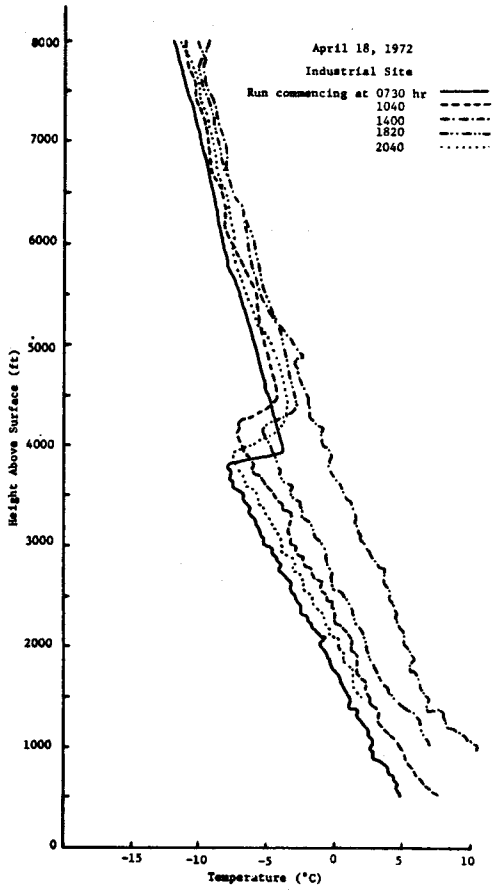

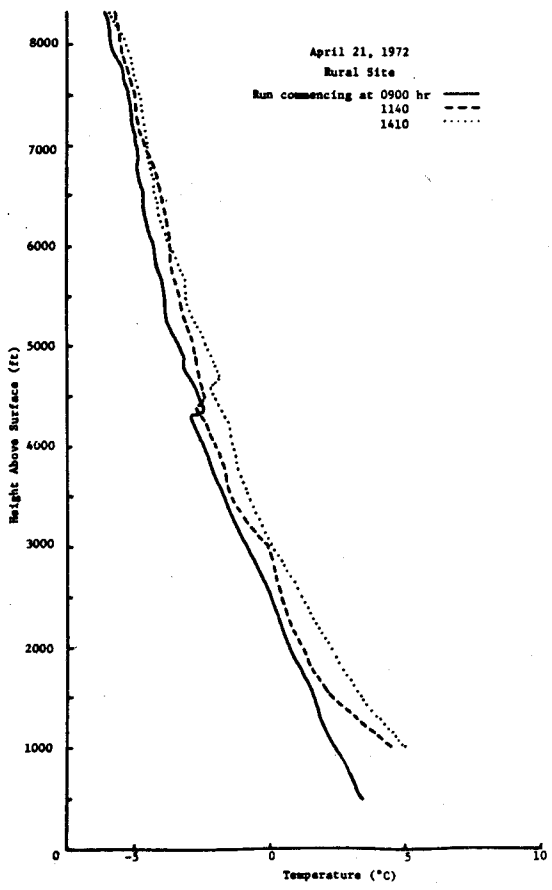

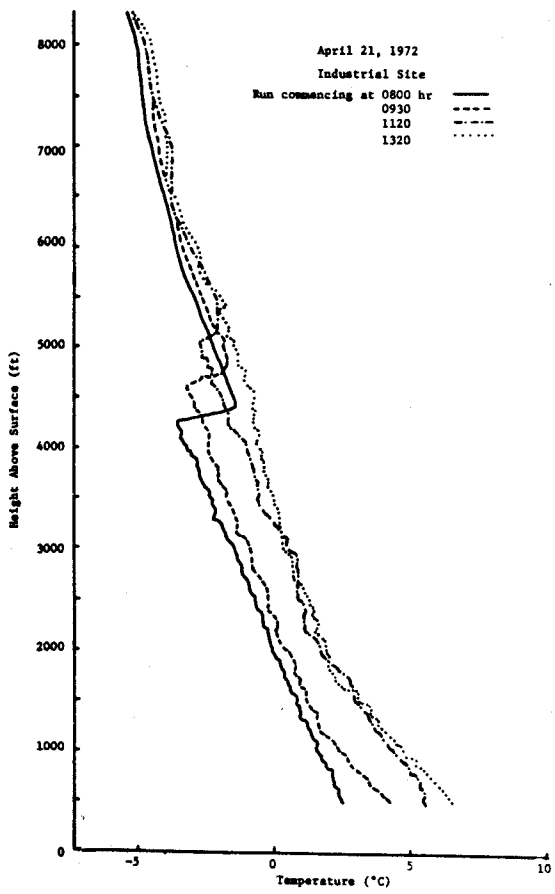

Figure 6 (continued)

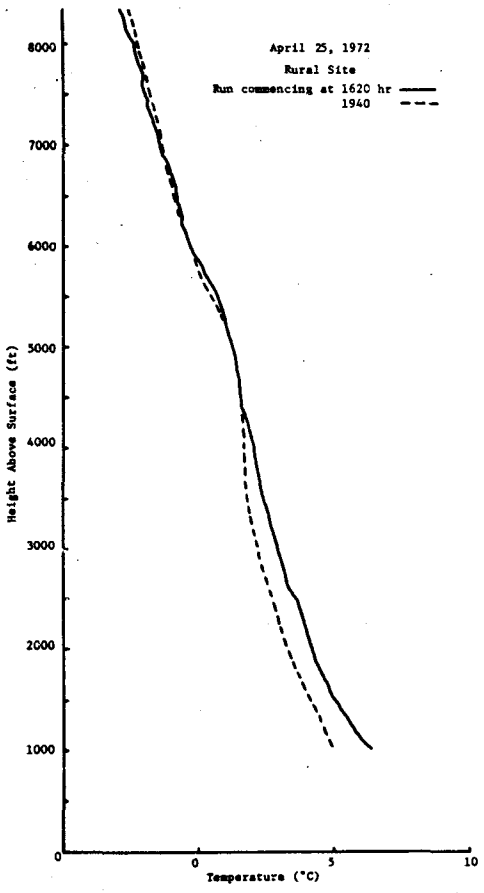

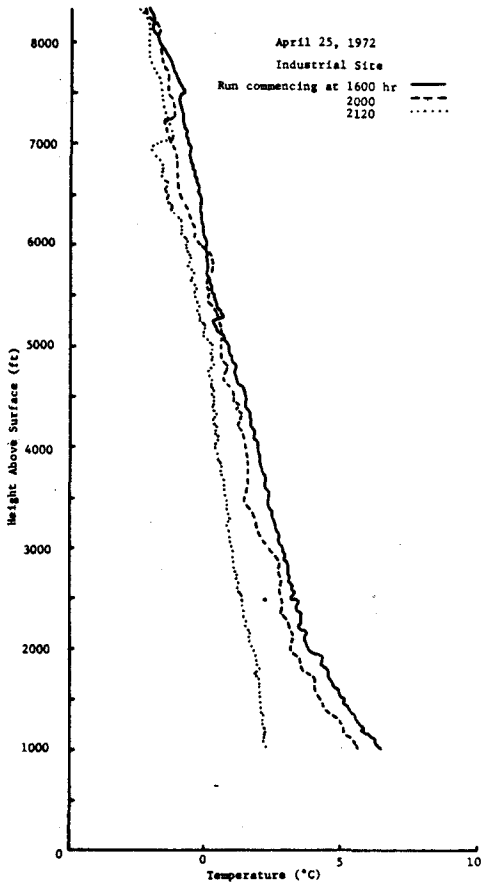

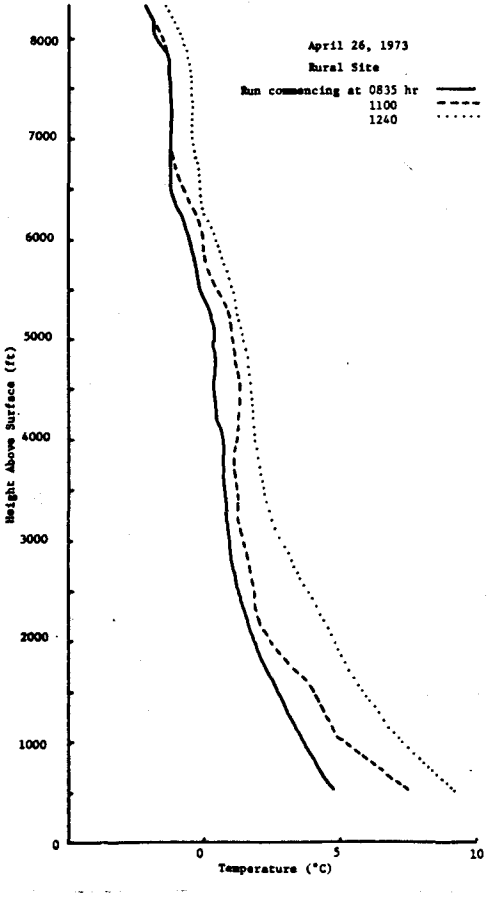

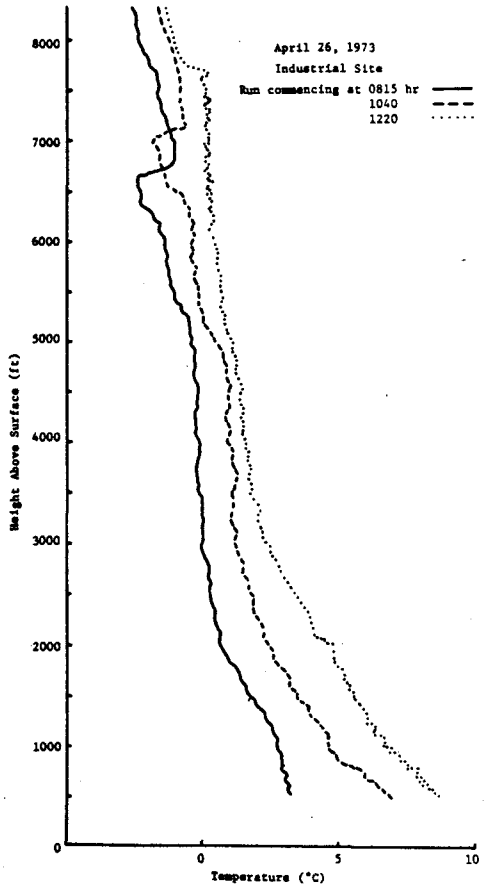

Figure 6 (continued)

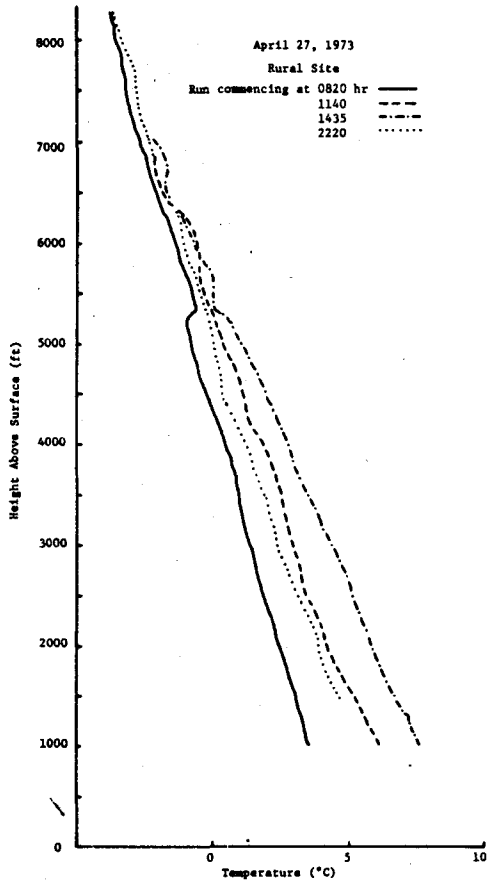

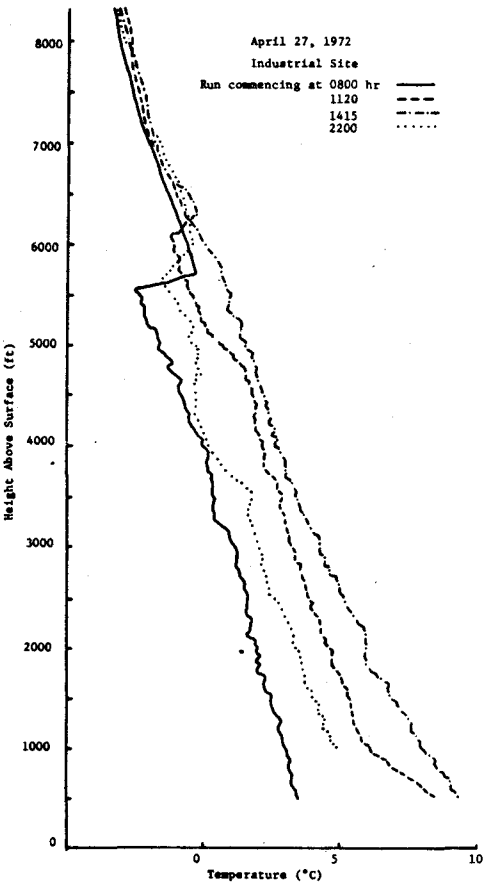

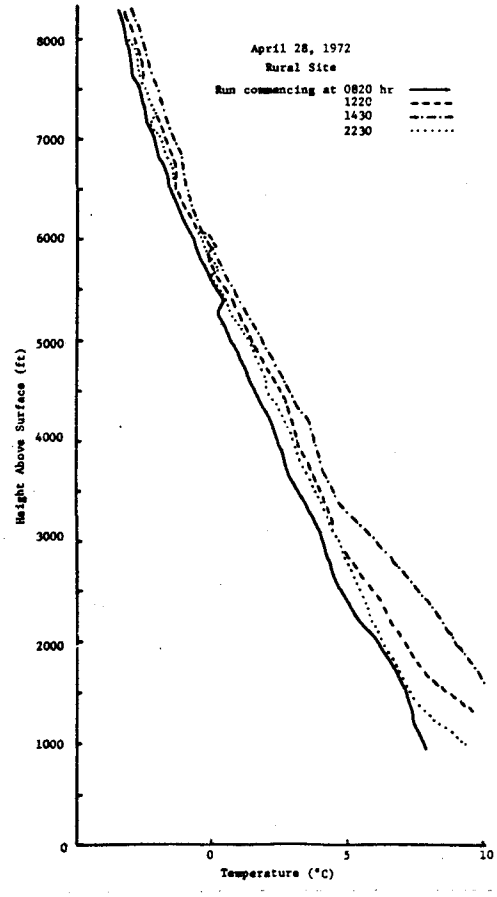

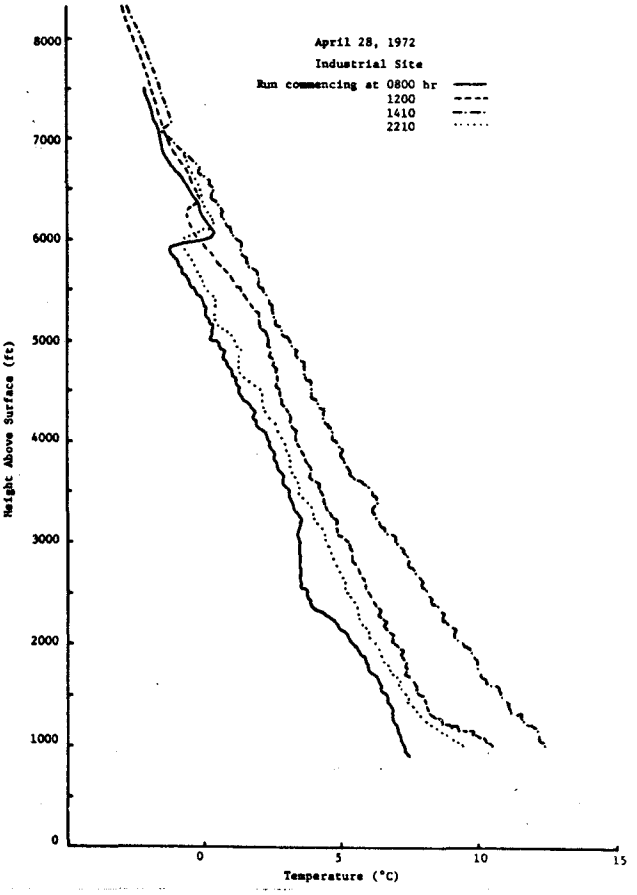

TABLE 3

RATES OF HEIGHT CHANGE FOR THE ELEVATED TEMPERATURE INVERSION AT THE INDUSTRIAL SITE

Date	Time of Day	Initial Height above Surface (ft)	Time (hour)	Rate of Change in Height Above Surface (feet/hr)	
Dec.22/71	Morning	3200	0945	260	
	Afternoon	4500	1445	-195	
Mar.10/72	Morning	3700	0840	150	
	Afternoon	4500	1400	-130	
Mar.27/72	Morning	4100	0800	230	
	Afternoon	5600	1430	-230	
Mar.28/72	Morning	4400	0830	110	
	Afternoon	5000	1400	- 75	
Apr.18/72	Morning	3900	0730	155	
	Afternoon	4900	1400	-135	
Apr.21/72	Morning	4300	0800	205	
Apr.25/72	Afternoon	7500	1600	- 97	
Apr.26/72	Morning	6700	0815	245	
Apr.27/72	Morning	5600	0800	110	
	Afternoon	6300	1415	- 65	
Apr.28/72	Morning	6000	0800	180	
	Afternoon	7100	1410	-125	
Average	Morning			183	/9
	Afternoon			-153	/8

TABLE 4

COMPARISON OF THE RATES OF TEMPERATURE CHANGE AT THE INDUSTRIAL AND CONTROL SITES FOR VARIOUS HEIGHTS ABOVE GROUND

Date	Time of Day	Height above Surface	Rate of Temperature Change (C°/hr)	
			Industrial Site	Control Site
December 22, 1971	Morning	1000	0.29	-
		2000	0.29	-
		3000	0.15	-
		4000	-	-
	Afternoon	1000	-	-
		2000	-0.21	-0.08
		3000	-0.41	-0.19
		4000	-	-0.08
March 10, 1972	Morning	1000	0.85	0.78
		2000	0.63	0.38
		3000	0.56	0.16
		4000	-	0.16
	Afternoon	1000	-1.12	-0.25
		2000	-0.56	-0.31
		3000	-1.12	-0.25
		4000	-	-0.12
March 27, 1972	Morning	1000	0.45	-
		2000	0.55	0.50
		3000	0.55	0.33
		4000	0.33	0.11
	Afternoon	1000	-0.39	-0.19
		2000	-0.39	-0.17
		3000	-0.39	-0.12
		4000	-0.35	-0.06
March 28, 1972	Morning	1000	0.79	0.73
		2000	0.73	0.64
		3000	0.73	0.57
		4000	0.66	0.30
	Afternoon	1000	-0.63	-0.35
		2000	-0.56	-0.63
		3000	-0.47	-0.51
		4000	-0.53	-0.24
April 18, 1972	Morning	1000	0.61	0.54
		2000	0.48	0.30
		3000	0.56	0.39
		3500	0.58	0.41

TABLE 4 (continued)

COMPARISON OF THE RATES OF TEMPERATURE CHANGE AT THE INDUSTRIAL AND CONTROL SITES FOR VARIOUS HEIGHTS ABOVE GROUND

Date	Time of Day	Height above Surface	Rate of Temperature Change (C°/hr)	
			Industrial Site	Control Site
April 18, 1972	Afternoon	1000	-	-
		2000	-0.36	-0.15
		3000	-0.45	-0.15
		3500	-0.35	-0.20
April 21, 1972	Morning	1000	0.40	0.47
		2000	0.37	0.29
		3000	0.37	0.17
		4000	0.49	00.22
April 25, 1972	Afternoon	1000	-0.80	-0.41
		2000	-0.40	-0.30
		3000	-0.33	-0.23
		4000	-0.31	-0.11
April 26, 1972	Morning	1000	0.92	0.89
		2000	1.01	0.70
		3000	0.58	0.46
		4000	0.43	0.28
April 27, 1972	Morning	1000	0.76	0.64
		2000	0.64	0.56
		3000	0.50	0.48
		4000	0.44	0.36
	Afternoon	1000	-0.40	-
		2000	-0.34	-0.26
		3000	-0.29	-0.26
		4000	-0.32	-0.21
April 28, 1972	Morning	1000	0.83	--
		2000	0.65	0.49
		3000	0.59	0.33
		4000	0.40	0.22
	Afternoon	1000	-0.37	-
		2000	-0.37	-0.34
		3000	-0.33	-0.19
		4000	-0.25	-0.09

TABLE 5

AVERAGE RATES OF TEMPERATURE CHANGE

Time of Day	Height above Ground (feet)	Rate of Temperature Change (C°/hour)	
		Industrial Site	Control Site
Morning	1000	0.66 / 9	0.68 / 6
	2000	0.59 / 9	0.48 / 8
	3000	0.51 / 9	0.36 / 8
	4000	0.48 / 7	0.26 / 8
	Overall	0.56 / 34	0.43 / 30
Afternoon	1000	-0.62 / 6	-0.30 / 4
	2000	-0.40 / 8	-0.28 / 8
	3000	-0.47 / 8	-0.24 / 8
	4000	-0.35 / 6	-0.14 / 8
	Overall	-0.46 / 28	-0.23 / 28

CHAPTER V

DISCUSSION

1. Radiation

The additional attenuation of shortwave radiation in the urban atmosphere is mainly attributable to the greater absorptive properties of the particulate matter suspended over the industrial area. Studies by Roach (1961) and Sheppard (1958) indicated that most radiation scattered by these particles is directed forward (Mie scattering) and thus attenuation of solar radiation is primarily due to absorption.

The additional energy absorbed by the urban/industrial atmosphere is reradiated in the form of longwave or infrared radiation. This radiation emission must be isotropic such that one half of the absorbed energy is re-emitted skyward and the other half is directed to the surface.

Observations indicate, however, that the quantity of incoming shortwave energy that is attenuated is almost exactly matched by the increase in longwave energy emitted by the atmosphere to the surface at the urban site. Only a maximum one-half of the increase in longwave emission can be accounted for by considering it as absorbed radiation that has been re-emitted. It is suggested here that the remaining portion of the increase in longwave emission to the surface is attributable to higher emissivities exhibited by particles in the urban atmosphere and also to their correspondingly higher longwave absorptivities. This permits the capture of some

outgoing longwave from the surface, half of which is re-emitted as incoming longwave.

The following argument is presented as an explanation of the observed phenomena:

The shortwave coefficient of attenuation, a, may be considered as

$$a = a_r + a_m + a_{abs}$$

where a_r is the coefficient of Rayleigh scattering,

a_m is the coefficient of Mie scattering, and

a_{abs} is the coefficient of absorption.

Since the major attenuating substance in the urban atmosphere is particulate matter, $a_r \simeq o$. Hence, the only scattering process that is operating is Mie scattering. However, the attenuation of (Q+q) due to Mie scattering will be considered negligible for the purposes of this analysis since most of the radiation is scattered in the forward direction. (Roach, 1961 and Sheppard, 1958), In the city then,

$$a = a_{abs}$$

Let $a(Q+q)$ be the additional quantity of incoming shortwave attenuated by the urban atmosphere before it reaches the surface.

Then,

$$a(Q+q) = \Delta \text{ internal energy of the atmosphere}$$
$$= k\, \partial T$$

where k is a constant and ∂T is the change in temperature.

The total longwave emission from the atmosphere, accounted for by temperature alone, is

$$E_T = \sigma \varepsilon_o T^4$$

where ε_o is the emissivity of a clean atmosphere.

The additional shortwave energy absorbed in the urban atmosphere will result in additional atmospheric heating in the pollution zone. The increase in temperature will, in turn, cause additional longwave emission as observations indicate. For an increase in temperature ∂T the increase in longwave emission will be

$$\frac{\partial E_T}{\partial T} = 4 \sigma \varepsilon_o T^3$$

$$\text{or} \quad \partial E_T = 4 \sigma \varepsilon_o T^3 \partial T,$$

where ∂E_T is the increase in longwave emission attributable to increased temperature alone.

Since radiation emission from suspended particles is isotropic (i.e. one half with an outgoing component and one half with an incoming component), the temperature difference does not account for all of the increase in longwave energy received at the surface in a pollution dome. Since only one half of ∂E_T is directed to the surface,

$$\partial E_T{\downarrow} = \frac{1}{2} a(Q+q)$$

where $\partial E_T{\downarrow}$ is that portion of the total increase in longwave emission (due to raised temperatures) which has an incoming component of direction.

In order that the increase in longwave emission to the surface can be equal to a(Q+q) as actually observed, it is postulated that an atmosphere containing particulate matter possesses an emissivity ε_p such that $\varepsilon_p > \varepsilon_o$ and

$$\partial E_{pT}{\downarrow} = 4\,\delta\,\varepsilon_p\,T^3\,\partial T = a(Q + q)$$

where $\partial E_{pT}{\downarrow}$ is the increase in longwave flux to the surface accounted for by a higher temperature and a higher emissivity.

An estimate of the magnitude of the industrial atmosphere's emissivity, relative to that of an unpolluted atmosphere, can be gained from the following example. On April 28, the temperature profile for 0820 hr. in the control atmosphere was the same as that for 0800 hr. in the industrial atmosphere. Using the Stefan-Boltzmann Law and assuming equal emissivities, the longwave emission from each atmosphere should be the same.

The incoming longwave radiation for the hour ending 0900 at the control site was 21.32 ly hr^{-1}. The longwave radiation received at the industrial site for the hour ending 0900 was 25.21 ly hr^{-1}. The radiating temperature of the atmosphere at both sites was, however, the same. Thus the emissivity of the industrial atmosphere relative to that of the control atmosphere is in the ratio of

$$\frac{\varepsilon_{ind}}{\varepsilon_{con}} = \frac{25.21 \text{ ly hr}^{-1}}{21.32 \text{ ly hr}^{-1}} = 1.18$$

Under the pollution conditions present between 0800 and 0900 hr.

on April 28, therefore, the emissivity of the industrial atmosphere exceeded that of the control atmosphere by 18%.

Nighttime measurements indicate that the incoming longwave radiation received at the industrial site is the same as that received at the control site. Since the emissivity of the urban/industrial atmosphere is higher than that of an unpolluted atmosphere, the main radiating body of air over the city must be cooler than that over the countryside at night in order to equalize the radiation emissions.

It is postulated that the nocturnal temperature profiles over the industrial and control sites take the form of those shown in Fig. 7. The urban "heat island" effect is preserved at the lowest levels, as is the ground-based inversion so often observed in rural areas at night (Davidson, 1967; Bornstein, 1968; Clarke, 1969). Of significance, however, is the fact that the main radiating body of air over the rural site is warmer than that over the urban area by night. This effect was noted by Davidson (1967) and Bornstein (1968) working in New York City, and by Clarke (1969) in Cincinnati. This finding is similar to that of Duckworth and Sandberg (1954) who noted a "crossover" of the urban and rural temperatures during several nighttime periods.

2. Air Temperature Profiles

The industrial profiles consistently exhibit a marked elevated temperature inversion during the nighttime hours. The pollution zone, which lies beneath the clean atmosphere, cools radiatively at a greater rate than the clean atmosphere above because of its higher emissivity. Consequently a substantial inversion is produced.

Figure 7

Proposed Nocturnal Air Temperature Profiles Above the Industrial and Control Sites

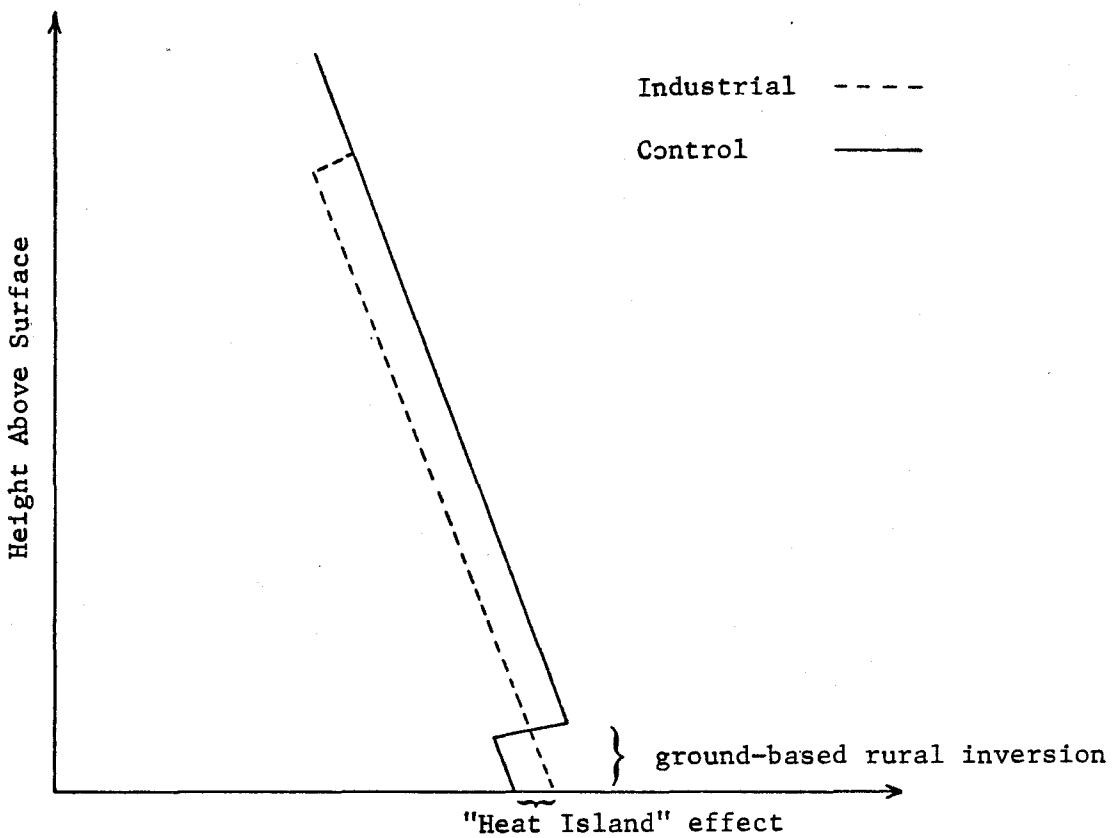

The temperature inversion becomes self-perpetuating because it traps additional pollutants injected into the atmosphere, which in turn reinforce the inversion itself. Visual observations indicate that the top of the inversion always coincides exactly with the top of the pollution dome. This suggests that the pollution dome and the pattern of air temperature behaviour within it are related.

The inversion diminishes in magnitude as the sunlight becomes more intense. The pollutants contained in the urban atmosphere are capable of absorbing considerably more shortwave radiation than clear air, resulting in a greater heating rate within the pollution dome than in the clear air above it. This is substantiated in Tables 4 and 5. The rates of temperature change at any height within the pollution dome nearly always exceed those measured over the control site at comparable heights.

About two hours after solar noon the inversion increases in magnitude. This increase continues beyond sunset. During this time the contaminated atmosphere cools at a rate greater than the control atmosphere because its radiative energy loss exceeds the energy input supplied by shortwave radiation absorption.

The elevated temperature inversion increases in height to a maximum about two hours after solar noon and descends again in the late afternoon. This rise and fall in height corresponds to the low and high solar zeniths with a phase lag of about two hours. The probable cause for such a phenomenon is convective buoyancy produced by atmospheric heating at the surface as well as within the pollution dome itself.

CHAPTER VI

CONCLUSIONS

The decrease in solar radiation intensity due to atmospheric pollution is balanced by a comparable increase in the flux of incoming longwave radiation from the sky. Thus the incoming all-wave radiation is the same whether the air is polluted or clear. For this to be so, the emissivity of the industrial atmosphere must exceed that of the control atmosphere.

Vertical air temperature profiles within the intense pollution layer differ markedly from those measured in a clean atmosphere. While the control profiles occasionally exhibit a weak subsidence inversion, the industrial profiles consistently show a marked inversion whose magnitude varies inversely with the intensity of incoming solar radiation, there being a phase lag of about two hours. This behaviour over the industrial area is attributed to the amplified shortwave absorptivity and longwave emissivity properties of the polluted atmosphere.

The height of the inversion increases during the morning hours and falls again during the later afternoon hours in response to atmospheric buoyant convection caused by surface and atmospheric heating during the day. The top of the inversion always coincides with the top of the pollution dome, indicating that the pollutants and the air temperature interact in a way that is self-perpetuating and maintains the pollution

dome.

Incoming longwave radiation at night is the same at the industrial and control sites. Since the emissivity of the industrial atmosphere is found to be greater than that of the control atmosphere, the main radiating body of air over the industrial site must be cooler than that over the control site. Evidence is presented from other studies which supports this claim.

BIBLIOGRAPHY

Atwater, M.A., 1971: Radiative effects of pollutants in the atmospheric boundary layer. J. Atm. Sci., 28(8), 1367-1373.

Bach, W., and W. Patterson, 1969: Heat budget studies in greater Cincinnati. Proc. Am. Assoc. Geog., 59, 7-11.

Bergstrom, R.W., 1971: The effects of urban air pollution on solar heating and turbidity. Conf. on air pollution meteorol., Rayleigh, N.C., 1971, Am. Meteorol. Soc., 93-97.

Bornstein, R.D., 1968: Observations of the urban heat island effect in New York City. J. Appl. Meteorol. 7(4), 575-582.

Clarke, J.F., 1969: Nocturnal urban boundary layer over Cincinnati, Ohio. Mon. Wea. Rev., 97, 582-589.

Conaway, J., and C.H.M. van Bavel, 1967: Radiometric surface temperature measurements and fluctuations in sky radiant emittance in the 600 to 1300 cm^{-1} waveband. Agron. J., 59(5), 389-390.

Davidson, B., 1967: A summary of the New York urban air pollution dynamics research program. J. Air Poll. Cont. Assoc., 17, 154-158.

Duckworth, F.S., and J.S. Sandberg, 1954: The effect of cities upon horizontal and vertical temperature gradients. Bull. Am. Meteorol. Soc., 35, 198-207.

East, C.C., 1967: Comparison du rayonnement solaire en ville et à la compagne. Paper presented to 35th Congress A.C.F.A.S., Sherbrooke.

Hand, I.F., 1949: Atmospheric contamination over Boston. Bull. Am. Meteorol. Soc., 30, 252-254.

Idso, S.B., 1972: Radiation fluxes during a dust storm. Weather, 27(5), 204-208.

Idso, S.B., and R.D. Jackson, 1968: Significance of fluctuations in sky radiant emittance for infrared thermometry. Agron. J., 60, 388-392.

Leighton, P.A., 1961: Photochemistry of Air Pollution. New York, Academic Press.

Lettau, H., and K. Lettau, 1969: Shortwave radiation climatonomy. Tellus, 21, 208-222.

Mateer, C.L., 1961: Note on the effects of the weekly cycles of air pollution on solar radiation at Toronto. Int. J. Air Water Poll. 4, 52-54.

Roach, W.T., 1961: Some aircraft observations of fluxes of solar radiation in the atmosphere. Quart. J. Roy. Met. Soc., 87, 346-363.

Robinson, G.D.,1962: Absorption of solar radiation by atmospheric aerosol as revealed by measurements at the ground. Arch. Met. Geophys. Biokl., B12, 19-40.

Rouse, W.R., and J.G. McCutcheon, 1972: The diurnal behaviour of incoming solar and infrared radiation in Hamilton, Canada. International Geography, 191-196.

Sekiguti, T., 1964: City climate distribution in and around the small city of Inas in central Japan, Tokyo Geog. Papers, 8, 93.

Sheppard, P.A., 1958: The effect of pollution on radiation in the atmosphere. Int. Jour. Air Poll., 1, 31-43.

Tebbens, B.D., 1968: Gaseous pollutants in the air. In Air Pollution, e.d. A.C. Stern. Vol. 1, 2nd Ed. New York, Academic Press, pp. 23-46.